

# TESTING PREDICTION CAPABILITIES OF AN $^{131}\text{I}$ TERRESTRIAL TRANSPORT MODEL BY USING MEASUREMENTS COLLECTED AT THE HANFORD NUCLEAR FACILITY

A. Iulian Apostoaei\*

**Abstract**—A model describing transport of  $^{131}\text{I}$  in the environment was developed by *SENES* Oak Ridge, Inc., for assessment of radiation doses and excess lifetime risk from  $^{131}\text{I}$  atmospheric releases from Oak Ridge Reservation in Oak Ridge, Tennessee, and from Idaho National Engineering and Environmental Laboratory in southeast Idaho. This paper describes the results of an exercise designed to test the reliability of this model and to identify the main sources of uncertainty in doses and risks estimated by this model. The testing of the model was based on materials published by the International Atomic Energy Agency BIOMASS program, specifically environmental data collected after the release into atmosphere of 63 curies of  $^{131}\text{I}$  during 2–5 September 1963, after an accident at the Hanford PUREX Chemical Separations Plant, in Hanford, Washington. Measurements of activity in air, vegetation, and milk were collected in nine counties around Hanford during the first couple of months after the accident. The activity of  $^{131}\text{I}$  in the thyroid glands of two children was measured 47 d after the accident. The model developed by *SENES* Oak Ridge, Inc., was used to estimate concentrations of  $^{131}\text{I}$  in environmental media, thyroid doses for the general population, and the activity of  $^{131}\text{I}$  in thyroid glands of the two children. Predicted concentrations of  $^{131}\text{I}$  in pasture grass and milk and thyroid doses were compared with similar estimates produced by other modelers. The *SENES* model was also used to estimate excess lifetime risk of thyroid cancer due to the September 1963 releases of  $^{131}\text{I}$  from Hanford. The *SENES* model was first calibrated and then applied to all locations of interest around Hanford without fitting the model parameters to a given location. Predictions showed that the *SENES* model reproduces satisfactorily the time-dependent and the time-integrated measured concentrations in vegetation and milk, and provides reliable estimates of  $^{131}\text{I}$  activity in thyroids of children. *SENES* model generated concentrations of  $^{131}\text{I}$  closer to observed concentrations, as compared to the predictions produced with other models. The inter-model comparison showed that variation of thyroid doses among all participating models (*SENES* model included) was a factor of 3 for the general population, but a factor of 10 for the two studied

children. As opposed to other models, *SENES* model allows a complete analysis of uncertainties in every predicted quantity, including estimated thyroid doses and risk of thyroid cancer. The uncertainties in the risk-per-unit-dose and the dose-per-unit-intake coefficients are major contributors to the uncertainty in the estimated lifetime risk and thyroid dose, respectively. The largest contributors to the uncertainty in the estimated concentration in milk are the feed-to-milk transfer factor ( $F_m$ ), the dry deposition velocity ( $V_d$ ), and the mass interception factor ( $r/Y$ )<sub>dry</sub> for the elemental form of iodine ( $\text{I}_2$ ). Exposure to the 1963 PUREX/Hanford accident produced low doses and risks for people living at the studied locations. The upper 97.5th percentile of the excess lifetime risk of thyroid cancer for the most extreme situations is about  $10^{-4}$ . Measurements in pasture grass and milk at all locations around Hanford indicate a very low transfer of  $^{131}\text{I}$  from pasture to cow's milk (e.g., a feed-to-milk transfer coefficient,  $F_m$ , for commercial cows of about  $0.0022 \text{ d L}^{-1}$ ). These values are towards the low end of  $F_m$  values measured elsewhere and they are low compared to the  $F_m$  values used in other dose reconstruction studies, including the Hanford Environmental Dose Reconstruction.

Health Phys. 88(5):439–458; 2005

**Key words:** environmental transport;  $^{131}\text{I}$ ; modeling, dose assessment; radiation, environmental

## INTRODUCTION

A MODEL describing transport of  $^{131}\text{I}$  in the environment was developed by *SENES* Oak Ridge, Inc., starting from first principles, and using basic equations, which are now standard in radiological assessment (Till and Meyer 1983). The model was designed for assessment of radiation doses and excess lifetime risk from releases of radioactivity from the Oak Ridge Reservation in Oak Ridge, TN (Apostoaei et al. 1999a, b) and from the Idaho National Engineering and Environmental Laboratory (INEEL) in southeast Idaho (Apostoaei et al. 2003a). These environmental dose reconstruction and risk assessment studies were performed to determine if epidemiologic studies or other public health activities should be undertaken and to inform members of the public about past exposures to radiation. To enhance the credibility of

\* *SENES* Oak Ridge, Inc., 102 Donner Drive, Oak Ridge, TN 37830.

For correspondence or reprints contact: the author at the above address, or email at iulian@senes.com.

(Manuscript received 14 April 2003; revised manuscript received 28 October 2004, accepted 27 December 2004)

0017-9078/05/0

Copyright © 2005 Health Physics Society

the Oak Ridge and INEEL dose reconstruction studies, it is important to test the reliability of *SENES*  $^{131}\text{I}$  environmental transfer model and to identify the main sources of uncertainty in estimated doses and risks.

An opportunity for a model testing exercise is offered by data collected after an accidental atmospheric release of about 2.33 TBq (63 Ci) of  $^{131}\text{I}$  from the Hanford PUREX Chemical Separations Plant, in Hanford, WA, during 2–5 September 1963. Measurements of  $^{131}\text{I}$  activity in air, vegetation, and milk collected in nine counties around Hanford for more than 1 mo after the accident have been compiled for the International Atomic Energy Agency's (IAEA) BIOMASS Program (Biosphere Modeling and Assessment Methods; IAEA 2003,<sup>†</sup> Thiessen et al. 2002; Thiessen et al. in press). The compiled data included activities of  $^{131}\text{I}$  in the thyroid glands of two children.

The BIOMASS Hanford Scenario was used to test the *SENES*  $^{131}\text{I}$  environmental transport model by comparing estimated concentrations in environmental media, thyroid gland burdens, and thyroid doses against measurements collected after the Hanford accident and against predictions produced by other models using the same data set. In addition to thyroid doses, the *SENES* model was used to estimate excess lifetime risk of thyroid cancer for people living around Hanford. The uncertainty in the estimated concentrations in environmental media, doses, and risks was quantified, and the components of the exposure pathways that contributed the most to the uncertainty in the doses and risk (e.g., deposition, interception by plants, transfer to milk, intake, dose coefficients, risk factors) were determined.

## BACKGROUND

The Hanford Scenario (IAEA 2003) provides a description of the Hanford area and vicinity (Fig. 1), gives details about the releases including local and regional meteorological data during the accident, and summarizes the monitoring data collected in the first month after the accident. An overview of this information is presented below.

The accidental release of  $^{131}\text{I}$  started on 2 September 1953, when 0.89 TBq (24 Ci) were lost into the atmosphere through a 60-m stack at the PUREX plant. An additional 1.26 TBq (34 Ci) were released on 3 September, 0.13 TBq (3.6 Ci) on 4 September, and 0.048 TBq

(1.3 Ci) on 5 September, for a total of 2.33 TBq (63 Ci). Minimal releases of iodine took place during the 6–11 September period (0.0037–0.015 TBq  $\text{d}^{-1}$  or 0.1–0.4 Ci  $\text{d}^{-1}$ ). About 0.26 TBq (7 Ci) of iodine were released from 12 September until the end of the month, due to either cleanup or due to resuming normal operations. A total of 2.66 TBq (72 Ci) was recorded during the entire month of September. This total amount was used to produce the doses and risks reported in this paper. About 90% of total amount of  $^{131}\text{I}$  was released before 6 September. The temperatures during these days varied between 16 and 21 °C (60 to 70 °F) during the night, and from 29 to 35 °C (85 to 95 °F) during the day. No rain event took place during these days in the area of interest, and vegetation was very dry.

The locations of the air measurement stations, farms, and cities relative to the PUREX plant stack are presented in Fig. 2. The scenario gives measurements of  $^{131}\text{I}$  concentration in air for each of the stations in Fig. 2. Measured concentrations of  $^{131}\text{I}$  in vegetation and milk are reported for 7 locations: Farm A—Benton City, Farm B—Twin Bridges, Farm K—Ringold, Farm T—Pasco, Farm N—Mesa, Farm Z—Eltopia, and Farm G—Byers Landing. The amount of iodine in the thyroids of two children living on Farm B was measured on 19 October 1963.

Predictions from seven other modelers (Table 1) are available for deposition of  $^{131}\text{I}$ , concentration of  $^{131}\text{I}$  in vegetation and milk at 6 locations (Farms A, B, K, N, T, Z), for thyroid burdens and dose for the two children at Farm B, and for  $^{131}\text{I}$  intake and thyroid doses for representative individuals at 6 locations (IAEA 2003; Thiessen et al. in press). A description of the main characteristics of the models used by each participant and a summary of some of the main parameter values used in these models are presented in IAEA (2003).

## METHODS

The Hanford Scenario requires prediction of short-term bioaccumulation of  $^{131}\text{I}$  after an acute release. The environmental transport model developed by *SENES* Oak Ridge, Inc., can be used to predict bioaccumulation in environmental media after acute or chronic releases of  $^{131}\text{I}$  (Apostoaie et al. 1999a).

In the exercise presented in this paper, calculations are started with concentrations of  $^{131}\text{I}$  in air obtained from other sources (i.e., measurements or atmospheric transport model predictions). Thus, only the terrestrial portion of the environmental transport model is tested in this paper. For many locations around Hanford, daily measurements of concentration of  $^{131}\text{I}$  in air ( $C_a$ ) during September 1963 were available, and they were used in

<sup>†</sup> The Hanford Scenario is available at <http://www-pub.iaea.org/MTCD/publications/publications.asp> (accessed on October 2004; search the IAEA publication list for keyword "Iodine-131"). The model testing data (i.e., scenario description, input data, test data; but no model predictions) are also available on the Centers of Disease Control and Prevention (CDC) Web site at: <http://www.cdc.gov/nceh/radiation/> (under "International Projects;" accessed October 2004).

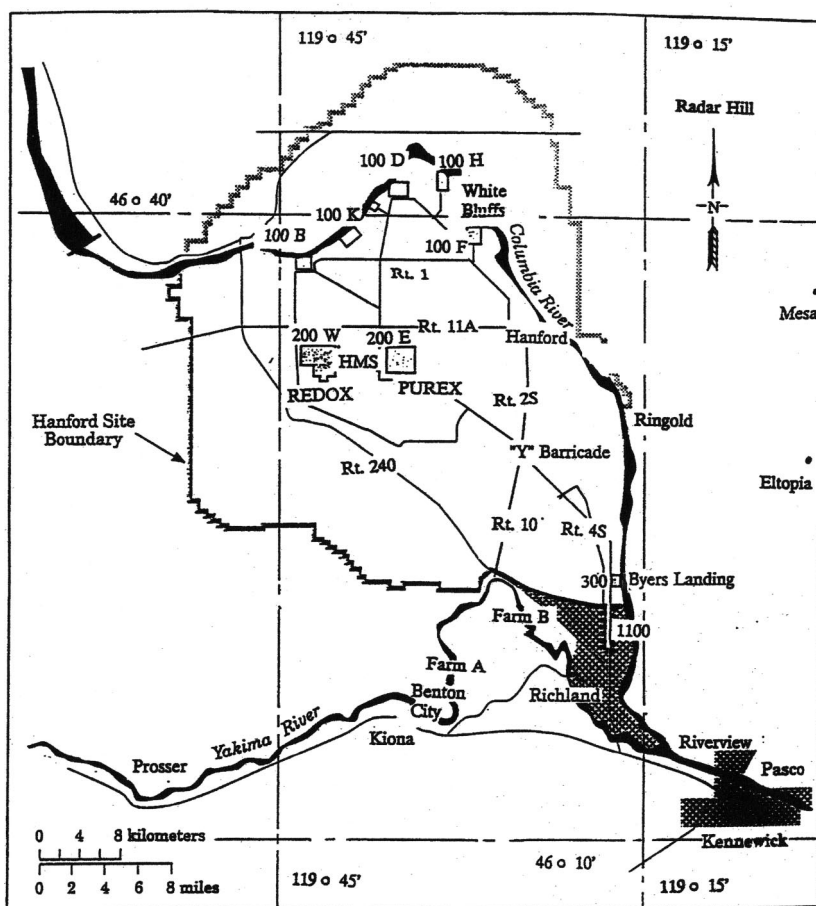


Fig. 1. Map of the Hanford reservation and its vicinity (reproduced from IAEA 2003).

calculations (Fig. 2). For locations where no air concentration measurements were available, the concentration of  $^{131}\text{I}$  in air was reconstructed based on previous estimates of total  $^{131}\text{I}$  deposition on the ground (as described later in the paper).

The concentration in pasture grass as a function of time ( $t$ ) after the accident is given by:

$$\frac{dC_{g,f}}{dt} = \dot{d} - \lambda_{\text{eff}} \times C_{g,f}, \quad (1)$$

where

- $C_{g,f}$  = concentration in pasture grass ( $\text{Bq kg}^{-1}$  fresh mass);
- $\lambda_{\text{eff}}$  = effective removal rate of  $^{131}\text{I}$  from the vegetation ( $\text{d}^{-1}$ ), and is given by the sum of the radiological decay rate ( $\lambda_R$ ;  $\text{d}^{-1}$ ) and the weathering removal rate ( $\lambda_w$ ;  $\text{d}^{-1}$ ); and
- $\dot{d}$  = deposition rate of  $^{131}\text{I}$  ( $\text{Bq d}^{-1} \text{ kg}^{-1}$  fresh mass).

The deposition rate is estimated from the concentration of  $^{131}\text{I}$  in air at each location ( $C_a$ ):

$$\dot{d} = C_a \sum_{k=1}^3 \alpha_k V_{d,k} \left( \frac{r}{Y} \right)_{\text{dry}, k} \gamma_{\text{dry-to-fresh}}, \quad (2)$$

where

- $C_a$  = concentration in air of total  $^{131}\text{I}$  (i.e., all physico-chemical forms) at each location of interest ( $\text{Bq m}^{-3}$ );
- $k$  = one of the three physico-chemical forms of  $^{131}\text{I}$  (elemental, particulate, organic) present in air at a given location;
- $\alpha_k$  = fraction of the amount of  $^{131}\text{I}$  that is present in air in physico-chemical form  $k$  (unitless);
- $V_{d,k}$  = total dry deposition velocity of  $^{131}\text{I}$  ( $\text{m d}^{-1}$ ) for physico-chemical form  $k$ ;
- $(r/Y)_{\text{dry}, k}$  = mass interception fraction ( $\text{m}^2 \text{ kg}^{-1}_{\text{dry mass}}$ ) per dry vegetation mass for physico-chemical form  $k$ ; and
- $\gamma_{\text{dry-to-fresh}}$  = dry-mass to fresh-mass conversion factor ( $\text{kg}_{\text{dry mass}} \text{ kg}^{-1}_{\text{fresh mass}}$ ).

Eqn (2) accounts for dry deposition of  $^{131}\text{I}$ . Wet deposition was neglected because no rain events occurred during the period of interest. The predicted concentration of  $^{131}\text{I}$  in grass per unit of fresh mass is used for comparisons with the reported measurements of  $^{131}\text{I}$  in grass. The concentration in milk at the time of

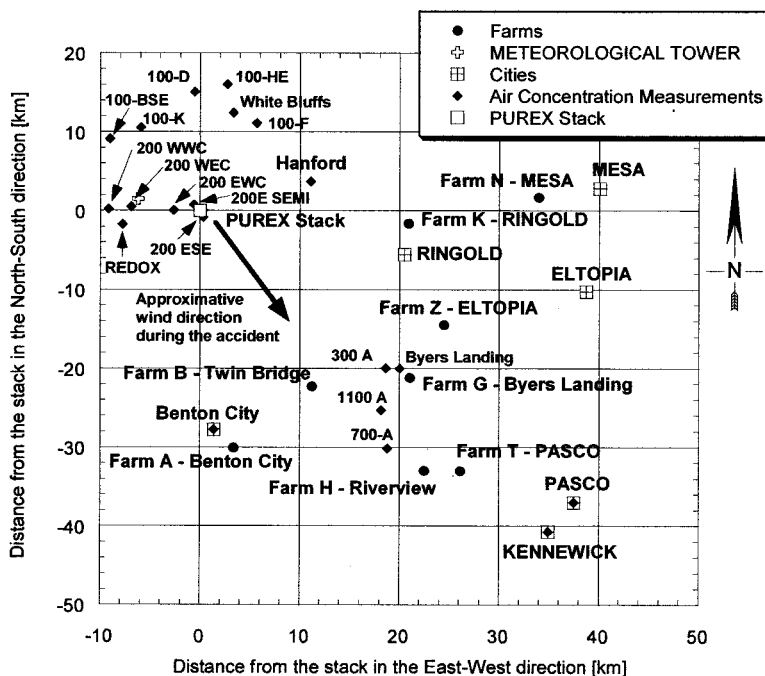


Fig. 2. Location of various landmarks relative to the Hanford PUREX stack ( $46^{\circ} 33' 0''$  North Latitude and  $119^{\circ} 31' 6''$  West Longitude; IAEA 2003).

Table 1. Modelers using the BIOMASS Hanford data (IAEA 2003; Thiessen et al. in press).

Modeler <sup>a</sup>	Country	Model
Napier, B.	USA	HEDR
Filistovic, V.	Lithuania	LIETDOS-FILTSEG
Homma, T. <sup>b</sup>	Japan	OSCAAR
Krajewski, P.	Poland	CLRP
Kryshev, A.	Russia	THYPHOON
Kanyar B./Nenyeci, A.	Hungary	TAMDYN
Tveten, U.	Norway	— <sup>c</sup>

<sup>a</sup> All modelers other than Krajewski estimated concentrations of  $^{131}\text{I}$  in air using atmospheric dispersion models. Krajewski estimated concentrations of  $^{131}\text{I}$  in air based on measured concentrations of  $^{131}\text{I}$  in air and vegetation. Most participants made predictions for five locations: Farm A—Benton City, Farm B—Twin Bridges, Farm T—Pasco, Farm N—Mesa, and Farm Z—Eltopia. Homma and Kanyar/Nenyeci also made predictions for a sixth location (Farm K—Ringold).

<sup>b</sup> Homma produced two sets of results: (1) using surface level and meso-scale (upper atmosphere) meteorological data from 12 meteorological stations, and (2) using only surface level meteorological data from a single meteorological station.

<sup>c</sup> A simple analytical approach was used, combined with atmospheric dispersion calculations using the MACCS model.

milking ( $C_m$ ) was calculated using the concentration in grass per dry mass and a standard feed-to-milk transfer coefficient ( $F_m$ ):

$$C_m = \frac{C_{g,f}}{\gamma_{\text{dry-to-fresh}}} \times Q_d \times F_m, \quad (3)$$

where

$C_m$  = concentration in milk at time of milking ( $\text{Bq L}^{-1}$ );

$Q_d$  = dry-mass feed ingestion rate ( $\text{kg d}^{-1}$ ); and  
 $F_m$  = feed-to-milk transfer coefficient ( $\text{d L}^{-1}$ ).

The estimated concentrations in grass and milk (at time of milking) were used for comparison with the values measured at selected locations.

The concentration in milk consumed by people ( $C_{mc}$ ) was estimated using the concentration in milk at milking ( $C_m$ ) multiplied by a factor accounting for radioactive decay during the period of time between milking and consumption. The intake rate of iodine from milk ingestion was obtained by multiplying the concentration in milk at consumption by a milk ingestion rate. It was assumed that all the milk consumed was obtained from local (i.e., contaminated) sources of milk:

$$INT_{\text{milk}} = C_m \times \exp(-\lambda_R \times T_{d,m}) \times U_m = C_{mc} \times U_m, \quad (4)$$

where

$C_{mc}$  = concentration of  $^{131}\text{I}$  in milk at the time of consumption by people ( $\text{Bq L}^{-1}$ );

$INT_{\text{milk}}$  = intake rate of  $^{131}\text{I}$  due to the ingestion of contaminated milk ( $\text{Bq d}^{-1}$ );

$\lambda_R$  = radioactive decay constant ( $\text{d}^{-1}$ );

$T_{d,m}$  = delay time between milking and consumption (d); and

$U_m$  = milk consumption rate ( $\text{L d}^{-1}$ ).

The total intake of <sup>131</sup>I for the month of September 1963 (*TINT*) was obtained by summing the daily intakes for each day of the month.

Similarly, the intake rate of <sup>131</sup>I from inhalation was estimated by multiplying the concentration of iodine in indoor and outdoor air by an inhalation rate and by a fraction of time spent indoors or outdoors, respectively:

$$INT_{INH,k} = [f_o + (1 - f_o)r_{io}] \times C_a \times \alpha_k \times BR, \quad (5)$$

where

$$\begin{aligned} INT_{INH,k} &= \text{intake rate from inhalation of } ^{131}\text{I in} \\ &\text{physico-chemical form } k \text{ (Bq d}^{-1}\text{);} \\ f_o &= \text{fraction of time spent outdoors (unitless);} \\ r_{io} &= \text{ratio of the indoor to outdoor concentra-} \\ &\text{tions of iodine in air (unitless);} \\ C_a &= \text{concentration of iodine in outside air (Bq} \\ &\text{m}^{-3}\text{air);} \\ \alpha_k &= \text{fraction of } ^{131}\text{I that is present in air in} \\ &\text{physico-chemical form } k \text{ (unitless); and} \\ BR &= \text{breathing rate for an individual (m}^3\text{air} \\ &\text{d}^{-1}\text{).} \end{aligned}$$

The uptake of each physico-chemical form of iodine into blood is calculated separately, by multiplying the intake by a fraction of iodine ( $D_k$ ) deposited in the respiratory tract and absorbed into blood:

$$INT_{INH,u} = \sum_{k=1}^3 INT_{INH,k} \times D_k, \quad (6)$$

where

$$\begin{aligned} INT_{INH,u} &= \text{activity of inhaled } ^{131}\text{I that is ultimately} \\ &\text{absorbed into blood (Bq d}^{-1}\text{); and} \\ D_k &= \text{fraction of the total amount inhaled that} \\ &\text{deposits in different parts of the respira-} \\ &\text{tory system and is absorbed into blood,} \\ &\text{for each physico-chemical form } k \text{ (unit-} \\ &\text{less).} \end{aligned}$$

Because practically 100% of the ingested iodine is absorbed into blood,  $INT_{milk}$  (eqn 4) represents the activity of <sup>131</sup>I transferred into blood by ingestion of milk. Similarly, the inhalation uptake rate ( $INT_{inh,u}$ ) represents the activity of <sup>131</sup>I transferred into blood by inhalation of <sup>131</sup>I.  $INT_{inh,u}$  and  $INT_{milk}$  can be summed into a combined intake rate, which is equivalent to a daily intake by ingestion needed to introduce into blood an activity numerically equal to ( $INT_{milk} + INT_{inh,u}$ ). Age-dependent thyroid doses from both ingestion and inhalation were estimated by using the combined intake rate and the dose coefficient for ingestion of <sup>131</sup>I (eqn 7). This approach avoids the use of dose coefficients for inhalation of <sup>131</sup>I for which uncertainties have not yet been fully quantified.

Also, this approach accounts for the correlations between the doses due to ingestion and those due to inhalation. When a person is inhaling and ingesting <sup>131</sup>I during the same period of time, the same physical and physiological parameters must be used in modeling internal doses from inhalation and ingestion (e.g., a low thyroid mass or a high absorption from blood to thyroid gland). That is, doses from inhalation and those from ingestion are correlated, and this correlation must be taken into consideration when uncertainties are estimated using Monte-Carlo methods. Ignoring this type of correlation leads to an underestimation of uncertainty in the total thyroid dose. The approach presented in this paper insures proper handling of correlations between ingestion and inhalation doses.

Thyroid doses from inhalation or ingestion of iodine were obtained by integrating the intake rates into a total intake and then multiplying by a dose coefficient representing the dose per unit intake:

$$D_a = TINT_a \times DCF_a, \quad (7)$$

where

$$\begin{aligned} D_a &= \text{thyroid dose given that the intake took} \\ &\text{place at age } a \text{ (Sv);} \\ TINT_a &= \text{total intake by ingestion, inhalation or total} \\ &\text{intake at age } a \text{ (in case of inhalation,} \\ &\text{INT}_{inh,u} \text{ defined above was used to deter-} \\ &\text{mine the total intake) (Bq); and} \\ DCF_a &= \text{thyroid dose coefficient (or dose conver-} \\ &\text{sion factor) representing the dose per unit} \\ &\text{intake at age } a \text{ (Sv Bq}^{-1}\text{).} \end{aligned}$$

The dose coefficients and their uncertainty were derived by using an internal dosimetry model (Apostoei et al. 1999a; Apostoei and Miller 2004) similar to the International Commission on Radiological Protection model (ICRP 1993), but based on more up-to-date measurements of the thyroid gland mass. The new measurements are obtained by ultrasound and indicate thyroid masses smaller than the thyroid masses obtained in the past by autopsy.

Excess lifetime risk of thyroid cancer was estimated using age-dependent risk factors (Land et al. 2003; Apostoei et al. 2003b):

$$ELR_a = D_a \times RF_a, \quad (8)$$

where

$$\begin{aligned} ELR_a &= \text{excess lifetime risk of thyroid cancer from} \\ &\text{an exposure at age } a \text{ (risk);} \\ D_a &= \text{thyroid dose from an intake at age } a \text{ (Sv);} \\ &\text{and} \end{aligned}$$

$RF_a$  = excess lifetime risk per unit dose for an exposure at age  $a$  (risk  $Sv^{-1}$ ).

Doses and risks from ingestion of contaminated milk and inhalation of contaminated air were calculated for representative individuals at six locations around Hanford (Farm A—Benton City, Farm B—Twin Bridges, Farm K—Ringold, Farm T—Pasco, Farm N—Mesa, Farm Z—Eltopia). The selected ages at exposure for the representative individuals are newborn, 1 y, 5 y, 10 y, 15 y, and adult (25 y).

Doses and risks were also calculated for the two real individuals exposed as children (a 4-y-old boy and an 8-y-old girl) while living on Farm B in the vicinity of the Hanford site. Thyroid burdens for the two children were estimated based on the ICRP biokinetic model for  $^{131}I$  (ICRP 1993; Apostoaei and Miller 2004), and they were compared to the activity measured on 19 October 1963, in the thyroid glands of these two children.

Parameter values and other modeling assumptions used in this testing exercise are discussed in the next section of the paper. Uncertainty in each parameter of the model was described using probability distribution functions (PDF). For each parameter's PDF, 400 samples were obtained using Latin Hypercube Sampling (LHS) technique (Iman and Shortencarier 1984; Morgan and Henrion 1990). LHS generates random samples that insure a more uniform sampling of the probability distribution functions, as compared to simple random sampling (e.g., clustering of samples are avoided, etc.), and, in particular, insure a better sampling at the limits of the distributions. The four hundred samples for each parameter were propagated simultaneously through the *SENES* model, and the resulting four hundred realizations of the estimated concentrations, doses, and risks were used to describe the uncertainties in these quantities.

The main contributors to the uncertainty in model predictions for each endpoint were determined using a sensitivity analysis based on a variance decomposition technique (Decisioneering 2000).

## MODEL ASSUMPTIONS AND PARAMETER VALUES

### Concentration of iodine in air

Measurements of  $^{131}I$  in air were taken at various permanent atmospheric monitoring stations maintained at Hanford (Fig. 1). Normally, these stations were equipped with "HV-70" brand filter and a caustic scrubber (Soldat 1965; IAEA 2003). The particulate filter was about 99.8% efficient in collecting particles with a 3- $\mu m$  diameter, and the caustic solution was reported to capture "most" of the molecular iodine. During September 1963,

the stations were supplemented by temporary caustic scrubbers and charcoal cartridge samplers, the latter being efficient in collecting organic iodine (Soldat 1965; IAEA 2003). Thus, the measurements of  $^{131}I$  in air are intended to represent the total  $^{131}I$  in air (i.e., in all chemical forms). The fraction of the total iodine that is either in molecular, particulate, or organic form is described in the next section.

**Farm A—Benton City.** The concentrations of  $^{131}I$  in air measured at Benton City were used to predict the concentrations and doses for Farm A (Fig. 1 and 2). Even though the two locations are close together and about the same distance from the accident plume centerline, the measured air concentration in Benton City is only partially relevant for Farm A. That is, due to local variations in the air movement patterns, the measured air concentration at the Benton City monitoring station can be higher or lower than the true average air concentration over the area of Farm A. In addition, the observed concentration of  $^{131}I$  in air at Benton City (as at any other location) is affected by measurement errors. The organizers of the exercise provided limited information regarding sample collection, preparation, and analytical methods, so the magnitude of measurement errors is not available. Given these two sources of uncertainty, the concentration of  $^{131}I$  in air for Farm A was judged to be equal to the concentration of  $^{131}I$  observed in Benton City, but with an uncertainty of a factor of 2. That is, the concentration for Farm A was defined as a lognormal distribution with a geometric mean equal to the observed concentration in Benton, and the 1st and 99th percentile equal to the observed concentration in Benton City divided and multiplied by 2, respectively.

**Farm B—Twin Bridges.** Farm B represents the location with the highest concentrations in grass and in milk, because it is very close to the plume centerline during the accident. The largest measured concentrations were reported at station 700-A, which was located few kilometers downwind from PUREX stack (Fig. 2). The air concentrations measured at station 700-A were used for Farm B, but with an uncertainty of a factor of 2 assigned to the air concentration to account for measurement errors and for the fact that the measurements could be only partially relevant for Farm B.

**Farm T—Pasco.** Farm T is downwind from the PUREX stack (Fig. 2). Measurements of  $^{131}I$  in air were taken in the cities of Pasco and Kennewick, which are further downwind from Farm T. In the first couple of days after the accident, the concentration of  $^{131}I$  in Kennewick was larger than in Pasco (0.23  $Bq\ m^{-3}$  vs.

0.096  $\text{Bq m}^{-3}$ , respectively). The next few days, the measured concentrations at the two locations were fairly similar (0.37  $\text{Bq m}^{-3}$  in Kennewick and 0.31  $\text{Bq m}^{-3}$  in Pasco). During the last half of September, the concentration in Kennewick was lower than the concentration in Pasco (0.067  $\text{Bq m}^{-3}$  vs. 0.11  $\text{Bq m}^{-3}$  during 18–24 September; and 0.011 vs. 0.037  $\text{Bq m}^{-3}$  during 25–30 September, respectively). For every day of September, the average of the measurements for Pasco and Kennewick was chosen to represent the concentration of  $^{131}\text{I}$  in air for Farm T, because Kennewick and Pasco stations were close enough to the geographical area of Farm T. Since the measurements were taken at a fixed point in space, while the farm represents a large area over which the concentration in air could have varied considerably, the average of the two measurements was judged to be the best representation of the average concentration for Farm T. As for Farms A and B, the uncertainty in the concentration in air for Farm T was assumed to be a factor of 2, accounting for the errors in extrapolation of measurements from one location to another, and for the inherent measurement errors.

**Farm K—Ringold.** No measured concentrations in air were available for Farm K or its vicinity. For this location, predictions were made starting from the total deposition previously estimated by other modelers (IAEA 2003). Two estimates of deposition at Ringold obtained with dispersion models were reported for Ringold. Of these two, one corresponds to an overestimate of the concentration in milk when compared to measurements at Ringold. A second estimate (Kanyar/Nenyai) led to a concentration in milk very close to the observed concentration (about 70% of the observation). Their reported estimate of total deposition was 43  $\text{Bq m}^{-2}$ , with a range from 34 to 60  $\text{Bq m}^{-2}$ . The predictions presented for Ringold in this paper are based on a total deposition of 50  $\text{Bq m}^{-2}$  (slightly higher than 43  $\text{Bq m}^{-2}$ ), with a range from 20 to 125  $\text{Bq m}^{-2}$  (triangular distribution). The range is based on the observation that, for other sites, the *SENES* model predicts total deposition from air concentrations with an uncertainty range of a factor of 2–2.5 above and below the central value. The back-calculated air concentration was assumed to have a time dependency similar to the one observed for Byers Landing (Figs. 1 and 2), which was the downwind location closest to Ringold for which  $^{131}\text{I}$  concentration in air was measured.

**Farm N—Mesa.** Concentrations of  $^{131}\text{I}$  in air were not measured in the vicinity of Farm N—Mesa, which is located about 34 km east of the PUREX plant. For this location, predictions were made starting from the total

deposition estimated by other modelers (IAEA 2003). There were 7 predictions made by 6 modelers, ranging from 6.5 to 356  $\text{Bq m}^{-2}$ , with an average of 68  $\text{Bq m}^{-2}$ . Most modelers predicted depositions lower than 68  $\text{Bq m}^{-2}$  with one participant producing a larger prediction. However, all modelers predicting the lower deposition values underestimated the time-integrated concentrations in pasture grass and milk. One of the closest sets of predictions for this location (Krajewski) was based on an estimated total deposition of 61  $\text{Bq m}^{-2}$ . Thus, a total deposition of 60  $\text{Bq m}^{-2}$  was used as a starting point for the model presented in this paper. Since the uncertainty in the total deposition produced by the *SENES* model for other locations was a factor of 2–2.5 around the central value, an uncertainty range of 25 to 140  $\text{Bq m}^{-2}$  (triangular distribution) was used for Farm N. The back-calculated air concentration was assumed to have the same time dependency as observed for Byers Landing (Figs. 1 and 2), which was the downwind location closest to Mesa for which  $^{131}\text{I}$  concentration in air was measured.

**Farm Z—Eltopia.** The scenario provided no air concentration measurements for Eltopia or its vicinity. Thus, the predictions reported in this paper are based on the total deposition estimated by other modelers (IAEA 2003). All seven modelers made predictions for Eltopia, with two predictions being very high (Homma and Tveten). Eliminating the two highest predictions, the estimated deposition for Farm Z ranged from 11 to 40  $\text{Bq m}^{-2}$  with an average of 26  $\text{Bq m}^{-2}$ . The predictions presented in this paper are based on a total deposition of 30  $\text{Bq m}^{-2}$ , with an uncertainty range of 10 to 75  $\text{Bq m}^{-2}$ . The back-calculated air concentration was assumed to have the same time dependency as observed for Byers Landing (Figs. 1 and 2), which was the location closest to Eltopia for which  $^{131}\text{I}$  concentration in air was measured.

### Transfer of iodine from air to vegetation and ground

**Chemical form of iodine.** Iodine was essentially released in molecular ( $\text{I}_2$ ) form (IAEA 2003). Molecular (or elemental) iodine is chemically reactive and during atmospheric transport it interacts with molecules in the air to form organic iodine compounds (e.g.,  $\text{CH}_3\text{I}$ ). Also, molecular iodine attaches to atmospheric aerosols. The scenario cites Ramsdell et al. (1994), who quantified the partition between these physico-chemical forms based on experiments that took place at or around the Hanford site. An experimental study was conducted at Hanford (Ludwick 1964) in which iodine was released into the atmosphere in elemental form. Measurements of different forms of iodine in the atmosphere indicated that

beyond a distance of roughly 3 km, 30% of iodine was in a particulate form, 36% was in an organic form, and the remaining 34% was in the elemental form. The same investigator (Ludwick 1967) also used measurements of  $^{131}\text{I}$  in stack gas and in air 5 miles downwind of the stack to estimate that the original iodine in elemental form partitioned into 15%, 43%, and 42% particulate, organic, and elemental forms, respectively. Ramsdell et al. (1994), after a review of several papers, concluded that the partitioning of iodine into different forms at 3.2 km in Ludwick's experiments (Ludwick 1964) was consistent with the results of other measurements of iodine in the plumes from other stacks at the Hanford site (Ludwick 1967; Perkins 1963, 1964), with the partitioning of iodine in the plume following the Chernobyl accident (Aoyama et al. 1986; Bondiotti and Brantley 1986; Cambray et al. 1987; Mueck 1988), and with the partitioning of natural iodine in the atmosphere (Voillequé 1979).

The scenario recommends a partitioning between the three physico-chemical forms of iodine as follows: 40% molecular (elemental) iodine, 20–60% organic iodine, and 2–25% iodine attached to particles (IAEA 2003). This recommendation seems to be reasonable given the experimental data presented above.

In this exercise, the fraction of iodine in molecular form was assumed to be distributed uniformly between 0.3 and 0.5 (with an average of 0.4), while the fraction of iodine in organic form was assumed to be uniformly distributed between 0.2 and 0.6 (with an average of 0.4). In each of the 400 Monte Carlo realizations, the fraction of iodine attached to particles was calculated as 1.0 minus the sum of the fractions for the other two chemical forms (1.0 – fraction molecular – fraction organic). Thus, in every realization, the sum of the molecular, particulate and organic fractions is 1.0. The fraction of particulate iodine was found to range from 0.05 to 0.43 (with a central value of 0.2).

**Dry deposition velocity.** Dry deposition was considered the dominant mechanism by which  $^{131}\text{I}$  was deposited onto the soil and on the surfaces of plants. Measurements of deposition velocities are reported by Chamberlain and Chadwick (1953, 1966), Chamberlain (1960) and Heinemann and Vogt (1980) and an analysis of the data is described by Apostoaei et al. (1999a). For this exercise, the dry deposition velocity for elemental (reactive) iodine was set to  $3.5 \text{ cm s}^{-1}$  with a range of 1 to  $6 \text{ cm s}^{-1}$ . For particulate iodine, the deposition velocity was taken as  $0.2 \text{ cm s}^{-1}$  with a range of 0.05 to  $0.5 \text{ cm s}^{-1}$ . Organic iodine is the least reactive of the three species and has the lowest deposition velocity ( $0.01 \text{ cm s}^{-1}$  with a range from 0.001 to  $0.05 \text{ cm s}^{-1}$ ). For each

physico-chemical form, a triangular distribution with the specified limits was used to describe the uncertainty in the dry deposition velocity.

**Mass interception factor.** On average, the ratio of the interception fraction to dry biomass is about  $2.1 \text{ m}^2 \text{ kg}^{-1}$  (dry mass) for pasture grass (yearly range is from 1.8 in summer to 2.3 in winter; Apostoaei et al. 1999a). This parameter can have a much larger variability for a short-term event such as the September 1963 accidental releases from Hanford. For gaseous iodine (i.e., elemental and organic) the mass interception factor  $(r/Y)_{\text{dry}}$  was set to  $2.2 \text{ m}^2 \text{ kg}^{-1}$  (dry mass) with a range from 0.8 to  $4 \text{ m}^2 \text{ kg}^{-1}$  (dry mass). Particulate iodine shows a slightly lower mass interception factor of  $2.0 \text{ m}^2 \text{ kg}^{-1}$  (dry mass), but the same uncertainty range was used (i.e., 0.8 to  $4 \text{ m}^2 \text{ kg}^{-1}$  dry mass). Triangular distributions with the specified limits were used to describe the uncertainty in the mass interception factor.

The product of the total dry deposition velocity ( $V_d$ ) and the mass interception factor  $(r/Y)_{\text{dry}}$  is called the normalized dry deposition velocity [ $V_D = V_d \times (r/Y)_{\text{dry}}$ ], and is experimentally obtained from the measured total deposition on grass ( $\text{Bq m}^{-2}$ ) divided by the measured time-integrated concentration in air at the location of the deposition ( $\text{Bq s m}^{-3}$ ), and the biomass of the vegetation ( $Y$ ). The normalized deposition velocity ( $V_D$ ) for elemental iodine obtained using the values for  $(V_d)$  and  $(r/Y)_{\text{dry}}$  listed above is  $6,600 \text{ m}^3 \text{ kg}^{-1} \text{ d}^{-1}$  (95% C.I. =  $2,500$ – $13,000 \text{ m}^3 \text{ kg}^{-1} \text{ d}^{-1}$ ). This range is included in the range of experimental values for  $V_D$  ( $700$ – $26,000 \text{ m}^3 \text{ kg}^{-1} \text{ d}^{-1}$ ) determined in an extensive set of iodine experiments performed at the Idaho National Engineering Laboratory in the 1960's in different weather conditions, as part of the Controlled Environmental Radioiodine Tests program (CERT) (Bunch 1966, 1968; Hawley et al. 1964).

**Dry-mass to fresh-mass conversion factor.** The Hanford area is generally very dry in late summer and early fall, and September 1963 was no exception. No important precipitation was recorded, and not even dew formed on the plants (the air temperature was greater than the dew point for most of the month, including the night of 2–3 September, when most of the iodine was released). Thus, it is expected that the standing vegetation was very dry. The authors of the scenario indicated that pasture grass had a content of 20–40% dry matter, while leafy weeds had as much as 60% dry matter (IAEA 2003). The dry-mass to fresh-mass conversion factor for pasture grass was set to  $0.33 \text{ kg}_{\text{dry}} \text{ kg}_{\text{fresh}}^{-1}$  with a range from 0.2 to  $0.45 \text{ kg}_{\text{dry}} \text{ kg}_{\text{fresh}}^{-1}$ . A uniform distribution was used to express the uncertainty in this parameter.

**Cow feeding regime and milk production.** The scenario provides site-specific information about the average amount of feed consumed by dairy cows during the fall season (IAEA 2003). Commercial dairy cattle consumed about  $8.5 \text{ kg}_{\text{dry weight}} \text{ d}^{-1}$  of pasture grass,  $1.5 \text{ kg}_{\text{dry weight}} \text{ d}^{-1}$  of grain supplement, and  $1.0 \text{ kg}_{\text{dry weight}} \text{ d}^{-1}$  of alfalfa hay. Family-owned (backyard) milk cows consumed about  $9 \text{ kg}_{\text{dry weight}} \text{ d}^{-1}$  of pasture grass and only about  $1.0 \text{ kg}_{\text{dry weight}} \text{ d}^{-1}$  of grain supplement. While the amount of pasture grass consumed by commercial and backyard cows is similar, commercial cows consume a larger total amount of feed than backyard cows, and, on average, commercial cows produce a larger amount of milk per day than backyard cows.

These feed intake rates are similar to those obtained in other studies and literature reviews (Koranda 1965; Hoffman and Baes 1979; Schwartz and Hoffman 1980; Miller 1996;<sup>‡</sup> NCI 1997). For instance, Koranda (1965) estimated a total ingestion rate of  $11.8 \text{ kg}_{\text{dry mass}} \text{ d}^{-1}$  for dairy cows managed in strip or rotational grazing systems, while for dairy cows grazing on open pastures (backyard cows), Koranda (1965) reported an average ingestion rate of  $9.1 \text{ kg}_{\text{dry mass}} \text{ d}^{-1}$ .

The above feeding rates are long-term averages of intake rates observed for many cows. Variability is expected in the ingestion rate for a given day or for a single cow. This variability is the source of uncertainty in the assigned ingestion rates. In this exercise, the pasture grass ingestion rate for commercial cows was assumed to vary from 7 to  $14 \text{ kg}_{\text{dry weight}} \text{ d}^{-1}$  with a central value of  $8.5 \text{ kg}_{\text{dry weight}} \text{ d}^{-1}$ . A triangular probability distribution was used to describe the uncertainty in this parameter. For backyard cows, a similar distribution was used, but the central value was set to  $9 \text{ kg}_{\text{dry weight}} \text{ d}^{-1}$  as indicated by the scenario.

## Transfer of iodine into milk

**Type of dairy cattle at various locations.** The authors of the scenario indicate that Farm B was a small farm with a few cows managed as “backyard” milk cows (IAEA 2003). However, larger dairy farms were located in the area east and southeast of Hanford, roughly bounded by Ringold, Eltopia, Pasco, Riverview, and Benton City (Figs. 1 and 2). These farms had dairy cattle managed for commercial production of milk and served as sources of milk for creameries in the regions.

A backyard cow consumes, on average, less feed than a commercial cow, but a higher fraction of feed consumed is pasture grass. Also, a backyard cow produces, on average, less milk than a commercial cow, but

it exhibits a higher transfer of  $^{131}\text{I}$  from feed to milk (i.e., larger  $F_m$ ). The differences in parameter values between the two types of cows are discussed in the following paragraphs. The predictions reported in this paper are made assuming that milk from Farm B was obtained from a single family-owned (backyard) cow, while the milk from all other farms was obtained from commercially managed cows, where milk from many cows was mixed.

**Transfer of iodine from feed to milk.** Values of the feed-to-milk transfer factor ( $F_m$ ) have been reviewed several times (Hoffman 1978; Hoffman and Baes 1979; Köhler et al. 1991; Snyder et al. 1994; NCI 1997; Apostoaei et al. 1999a) and have been the subject of an expert elicitation exercise (Brown et al. 1997). The feed-to-milk transfer factor for dairy cows does not vary substantially with breed of cow or with the level of iodine intake by cows. The  $F_m$  transfer factor is generally higher in the later stages of lactation, but this effect is not evident in the mixed milk from a dairy herd (NCI 1997). Lengemann et al. (1957) found pronounced seasonal changes in the  $F_m$  values. The highest transfer to milk was observed in spring and early summer, while the transfer was low in early fall and during the winter. The method used to measure the feed-to-milk transfer factor ( $F_m$ ) has an influence on the observed values. The highest transfer to milk was observed if encapsulated iodine was given to the cows. The lowest transfer is observed for the combined measurements of  $F_m$  values after the U.S. and global nuclear weapons testing, after the Chernobyl accident, and from controlled releases from nuclear power plants and nuclear fuel processing facilities (NCI 1997). Transfer factors determined from field tracer experiments have intermediate values.

Production of milk per milk cow in Washington State during the 1960's was about  $4,060 \text{ kg}$  per year (excluding milk sucked by calves; IAEA 2003). Given that the density of milk is close to unity (i.e.,  $1.03 \text{ kg m}^{-3}$ ) the milk production of a commercial cow was larger than  $11 \text{ L d}^{-1}$ . According to data analyzed by Apostoaei et al. (1999a), cows producing more than  $10 \text{ L}$  of milk per day can be considered high milk producers, and it is expected that they will exhibit a lower feed-to-milk transfer of iodine than the low milk-producing cows (i.e., those producing less than  $10 \text{ L d}^{-1}$ ).

Given that the studied releases came from a nuclear fuel processing facility and took place in early fall, a lognormal distribution with a geometric mean (GM) of  $0.003 \text{ d L}^{-1}$  was used for the  $F_m$  parameter for commercial cows. For backyard cows, the  $F_m$  parameter was also assumed to be lognormally distributed but with a higher GM ( $0.006 \text{ d L}^{-1}$ ) because backyard cows are generally

<sup>‡</sup> Private communication, Miller JK, University of Tennessee, Knoxville, Tennessee; February 1996.

low milk producers. Since the commercial milk consumed by humans is mixed from many cows, the average  $F_m$  should have a lower variability (i.e., GSD = 1.6) than the  $F_m$  for the milk from single backyard cows (i.e., GSD = 1.9). These values are relatively low compared to the values normally used in other dose assessments (Snyder et al. 1994; NCI 1997; Apostoaei et al. 1999a), but they produce model predictions that compare well with the observed values.

### Intake of iodine by humans

**Delay time from collection to consumption.** For people drinking milk from backyard cows or goats, a minimum delay time between milking and human consumption is usually about 8 h (0.33 d). This is the time required for the fresh milk to cool down (Simon et al. 1990). The upper limit of the holdup time was chosen to be about 2 d, since people having access to a family cow or goat prefer to consume the milk fresh, and given that refrigeration, though already common in urban areas by 1963, may have not been available to all people around Hanford (Krasner-Khait 2000). For the delay between milking and consumption for backyard cow's milk ( $T_{d,m}$ ), a uniform distribution between 0.33 and 2 d was assumed.

For milk from commercial dairies, at least 1 d is necessary for transportation of milk from the producer to the consumer. The minimum time before consumption was probably about 1 d, in cases when fresh milk was delivered directly from farms by the milkman and consumed the same day. Since refrigeration systems were quite common in farms and grocery stores in the early 1960's (Krasner-Khait 2000), commercial milk could have been safely stored for 3 to 4 d, and then consumed within 1 or 2 d from the day of purchase. As a result, some individuals might have consumed milk up to 6 d after milking. A triangular distribution with a minimum of 1 d, a mode of 3 d, and a maximum of 6 d was assumed for the delay time between milking and consumption for commercial milk ( $T_{d,m}$ ).

**Milk consumption rates.** Milk ingestion rates relevant to the early 1960's in Washington State are reported by NCI (1997). Consumption of milk is the same for males and females less than 10 y of age, but teenage and adult females consume less milk than males of the same age (Table 2). The consumption rates for adults are significantly lower than the rates for children and teenagers.

**Inhalation parameters.** Exposure to the iodine present in air occurred over 1 mo. The concentration of

**Table 2.** Consumption rates of cow milk for representative individuals.

Age (y)	Milk ingestion rate (L d <sup>-1</sup> )		
	Males		
	Min <sup>a</sup>	Likeliest <sup>a</sup>	Max <sup>a</sup>
0.5–1 <sup>b</sup>	0.20		0.8
1–4	0.25	0.50	1.0
5–9	0.3	0.70	1.0
10–14	0.3	0.70	1.0
15–20	0.3	0.70	1.0
Adult	0.15	0.35	0.7
Age (y)	Females		
	Min <sup>a</sup>	Likeliest <sup>a</sup>	Max <sup>a</sup>
0.5–1 <sup>b</sup>	0.20		0.8
1–4	0.25	0.50	1.0
5–9	0.3	0.70	1.0
10–14	0.3	0.60	0.9
15–20	0.25	0.50	0.8
Adult	0.1	0.20	0.5

<sup>a</sup> To describe the uncertainty in the ingestion rates, a uniform distribution between the minimum and the maximum value was used for infants. A triangular distribution with the specified parameters was used for all other age groups.

<sup>b</sup> The values in the table represent an average consumption of cows' milk by infants 6 to 12 mo old. Newborns generally consume mother's milk (which is much less contaminated than cows' milk) or canned milk (which is considered uncontaminated by the Hanford 1963 release).

<sup>131</sup>I in air was determined by measuring the amount of <sup>131</sup>I accumulated on various filters during 2, 3, 4, and even 5 d of air sampling. Thus, the available air concentrations represent averages over long periods of time (i.e., greater or equal to 24 h). During such periods of time an individual had various activities (e.g., sleep, school, recreation, work, etc.) that required different rates of breathing. NCI (1997) derived average breathing rates by combining the ventilation rates for generic types of activity and the time allocated on average to such activities. The breathing rates (in m<sup>3</sup> d<sup>-1</sup>) for both males and females are 3.5, 7, 12, and 17 for age-groups 0, 1–4, 5–9, and 10–14 y, respectively (Table 3). For individuals 15–19 y and for adults, the rates differ by sex. For males, the rates are 19 and 23 m<sup>3</sup> d<sup>-1</sup>, respectively, while for females 18 m<sup>3</sup> d<sup>-1</sup> was used for both the 15–19 y and adult age groups. Lognormal distributions were used to describe the uncertainty in these parameters, with a geometric mean (GM) equal to the values listed above and with a geometric standard deviation (GSD) of 1.4.

**Fraction of time spent outdoors.** The amount of time that an individual spends outdoors is highly dependent on sex, age, lifestyle, and weather. No important precipitation was recorded during September 1963, and the temperature varied from 60°F at night to 90°F in the afternoon. Statistics on this parameter are sparse and practically nonexistent for the late 1940's and early

**Table 3.** Parameters used in the estimation of thyroid dose and risk due to inhalation of  $^{131}\text{I}$ .

Parameter	Units	Distribution			
	units	Fraction of time spent outdoors		mode	shape
		lower	upper		
$f_0$ —age 0–4	unitless ( $\text{h d}^{-1}$ )	0.02 (0.5)	0.21 (5.0)	0.05 (1.2)	triangular
$f_0$ —age 4–15	unitless ( $\text{h d}^{-1}$ )	0.063 (1.5)	0.29 (7.0)	0.21 (5.0)	triangular
$f_0$ —age 15+	unitless ( $\text{h d}^{-1}$ )	0.063 (1.5)	0.42 (10.0)	0.33 (8.0)	triangular
		Ratio of indoor to outdoor concentrations			
$r_{io}$ —(gases)	unitless	0.3	0.9	0.8	triangular
$r_{io}$ —(particles)	unitless	0.4	0.9	0.8	triangular
		Breathing rates			
		GM <sup>a</sup>	GSD <sup>a</sup>		
Newborn	$\text{m}^3 \text{d}^{-1}$	3.5	1.4		lognormal
1–4	$\text{m}^3 \text{d}^{-1}$	7	1.4		lognormal
5–9	$\text{m}^3 \text{d}^{-1}$	12	1.4		lognormal
10–14	$\text{m}^3 \text{d}^{-1}$	17	1.4		lognormal
15–19—males	$\text{m}^3 \text{d}^{-1}$	19	1.4		lognormal
15–19—females	$\text{m}^3 \text{d}^{-1}$	18	1.4		lognormal
Adult males	$\text{m}^3 \text{d}^{-1}$	23	1.4		lognormal
Adult females	$\text{m}^3 \text{d}^{-1}$	18	1.4		lognormal

<sup>a</sup> GM = geometric mean; GSD = geometric standard deviation.

1950's; thus, professional judgment was used to define the values for this parameter (Table 3). For children less than 4 y of age, the distribution for the fraction of time spent outdoors was chosen to be a triangular distribution with a most likely value of 0.05. This represents an average of 1.2 h per day. The values for this age group range from 0.02 (half an hour per day) to 0.2 (about 5 h per day). For children 4 to 15 y old, the distribution is also triangular, with a most likely value of 0.21 (about 5 h a day) and a range of values from 0.063 (about 1.5 h per day) to 0.29 (about 7 h per day). Adults spend time outdoors or indoors according to their occupation. Workers in rural areas spend about 10 h outdoors every day (a fraction equal to 0.42). On the other hand, elderly people or housewives taking care of small children spend at least 1.5 h outside (a fraction equal to 0.063 of the year). For adults, a triangular distribution was selected with a minimum of 0.063, a maximum of 0.42, and a mode of 0.33 (8 hours a day).

**Indoor to outdoor concentration ratio.** The air inside a building is expected to have a different concentration of  $^{131}\text{I}$  than the air outside the building, unless free air exchange occurs through open windows or doors. When windows and doors are closed, some air is still exchanged between indoors and outdoors, either naturally through openings due to imperfect sealing or by a ventilation system. Ventilation systems were not well developed during the early 1960's. Air exchange by window or door opening was probably a common practice, especially during warm weather.

The concentration of a contaminant in indoor air is a function of the rate at which the contaminant is entering the building from the outdoor air, the rate of indoor

production of the contaminant (not an issue for  $^{131}\text{I}$ ), and the rate at which the contaminant is leaving the building. A summary of various studies performed to determine a relationship between outdoor and indoor air concentrations indicate that the ratio of the indoor to outdoor concentrations of iodine in air ( $r_{io}$ ) varies from 0.3 to 1 for gases, and from 0.4 to 1 for aerosols (Apostoaie et al. 1999a). Given the relatively warm weather and the lack of rain in September 1963, it is highly probable that many individuals would have kept their windows open, and free exchange between outdoor and indoor air was possible in many homes.

Triangular distributions with a mode of 0.8 (80%) and upper limits of 0.9 (90%) have been chosen for the indoor-to-outdoor ratio. The lower limit for elemental and organic iodine was set to 0.3 and for particulate iodine to 0.4.

### $^{131}\text{I}$ dosimetry

**Dose coefficients for ingestion of  $^{131}\text{I}$ .** A set of doses per unit intake (i.e., dose coefficients) and associated uncertainties was derived by Apostoaie and Miller (2004) for ingestion of  $^{131}\text{I}$  using the ICRP biokinetic model and the most recent summary of measurements of thyroid mass obtained by ultrasonography. The dose coefficients were described by lognormal distributions with the medians and the geometric standard deviations shown in Table 4.

**Dose coefficients for inhalation of  $^{131}\text{I}$ .** Dose coefficients for inhalation of iodine are reported by ICRP publications (e.g., ICRP 1996, 2000), but uncertainties in these coefficients are not well quantified. In this study,

**Table 4.** Age-specific thyroid dose coefficients ( $\times 10^{-7}$  Sv Bq $^{-1}$ ) for ingestion of  $^{131}\text{I}$  (Apostoaie and Miller 2004).

Age at exposure	Used in this study			Mean	GSD	ICRP <sup>a</sup> (2000)
	95% confidence interval	Lower limit	Median			
Infant	15	39	118	47	1.8	37
1	10	36	105	41	1.7	36
5	8.5	23	65	27	1.7	21
10	4.8	12	36	14	1.7	10
15	2.5	6.5	16	7.4	1.7	6.8
20 (males)	1.6	4.7	12	5.5	1.6	
Adult (males) <sup>b</sup>	1.6	4.2	11	4.8	1.6	4.3
20 (females)	1.9	5.0	13	5.9	1.6	
Adult (females) <sup>b</sup>	1.7	4.9	12	5.7	1.6	4.3

<sup>a</sup> The dose coefficients reported by ICRP (2000) are presented for comparison purposes.

<sup>b</sup> The values for adults were obtained for age at exposure 25 y, but they are applicable to adults exposed at ages  $\geq 25$ .

we made use of the fact that, after inhalation, all iodine deposited in the lungs is essentially transferred into blood. Similarly, ingested iodine is rapidly and almost totally transferred from the gastrointestinal tract into blood. Thus, the ingestion dose coefficients are representative for the dose per unit activity introduced into blood. Doses from inhalation can be estimated using ingestion dose coefficients multiplied by the intake by inhalation, and multiplied by the fraction of  $^{131}\text{I}$  deposited and absorbed in the respiratory system (see eqns 6, 7, and 8 and the afferent discussion). This approach makes use of the known uncertainties in ingestion dose coefficients (Apostoaie and Miller 2004) and accounts for correlations between doses due to ingestion and those due to inhalation.

In the case of releases from Hanford, iodine was released primarily in elemental form (IAEA 2003). During atmospheric transport, some of the elemental iodine attaches to particles already existing in the atmosphere and some is transformed into organic iodine. By the time the plume arrives at the downwind location where iodine is inhaled, the fraction of iodine in organic and particulate form will be appreciable. Most particles will have small or very small sizes ( $< 1 \mu\text{m}$ ) and are more likely to be of type *F*, rather than type *M* or type *S* (using the most recent ICRP 1996 absorption classes).

We performed a comparison between the thyroid dose factors for ingestion presented in ICRP Publication 67 (ICRP 1993) and the thyroid dose factors for inhalation derived from ICRP Publication 72 (ICRP 1996), which are based on the new ICRP lung model and contain the effect of partial deposition and absorption of  $^{131}\text{I}$  in the respiratory tract. ICRP Publication 67 reports ingestion dose factors based on 100% absorption of iodine.

The comparison was performed by taking the ratios between the inhalation dose coefficients (based on the newest lung model) and the ingestion dose coefficients (no deposition or absorption in the respiratory tract). Once iodine reaches the blood, the metabolism and

dosimetry is similar in the two ICRP publications. Thus, the estimated ratios are an indicator of the overall effect of the deposition and absorption of  $^{131}\text{I}$  as incorporated in the new lung model. For elemental iodine the ratio was 0.9, and for organic iodine the ratio was 0.7. For the fast absorbing particles ( $f_1 = 1$ ), the ratio was 0.4, and for the medium absorbing particles ( $f_1 = 0.1$ ), the ratio was 0.1.

Based on this comparison and on information about iodine deposition summarized by Apostoaie et al. (1999a), the following distributions were used for the fraction of iodine deposited and absorbed in the respiratory tract ( $D_i$ ):

- for elemental iodine—a uniform distribution between 0.8 and 1.0 (central value 0.9);
- for particulate iodine—a triangular distribution between 0.1 and 0.8 with a mode of 0.4; and
- for organic iodine—a uniform distribution between 0.6 and 0.8 (central value 0.7).

### Risk factors

The risk factors represent the excess lifetime risk (ELR) of thyroid cancer incidence per unit dose to the thyroid gland (ELR Sv $^{-1}$ ), based on a pooled analysis of studies of patients exposed to x rays and the Japanese A-bomb survivors study (Table 5; Land et al. 2003; Apostoaie et al. 2003b). A dose and dose-rate effectiveness factor (DDREF) was used to account for the fact that the  $^{131}\text{I}$  energy is deposited in the thyroid gland chronically and non-uniformly, over many days after intake.

## RESULTS AND DISCUSSION

### Predicted concentrations in pasture grass and milk

An initial set of predictions for Farm A (Benton City) was produced using the *SENES* model operated with the parameter values calibrated for the Oak Ridge, TN, region, which are considered default for this model. The initial predictions reproduced very well the measured time-dependent and time-integrated concentration

**Table 5.** Excess lifetime risk of thyroid cancer for 1 Sv dose to the thyroid (risk factors; ELR Sv<sup>-1</sup>; Land et al. 2003; Apostoaei et al. 2003b).

Age-group (y)	Risk factors (ELR Sv <sup>-1</sup> )			
	Males		Females	
	GM <sup>a</sup>	GSD <sup>a</sup>	GM <sup>a</sup>	GSD <sup>a</sup>
Infant	0.017	2.4	0.041	2.4
1	0.015	2.4	0.037	2.4
5	0.011	2.2	0.028	2.2
10	0.0074	2.2	0.018	2.2
15	0.0048	2.4	0.012	2.4
25 (adult)	0.0020	2.6	0.0048	2.6
4-y-old boy	0.0123	2.2		
8-y-old girl			0.021	2.2

<sup>a</sup> The uncertainty in the risk factors is described by lognormal distributions with the specified geometric mean (GM) and geometric standard deviation (GSD).

in milk, but underestimated the concentration in grass by a factor of about 3. The parameters of the model were adjusted by analyzing the information provided in the scenario and reported measured values, as discussed below.

The measurements show relatively high concentrations of <sup>131</sup>I in pasture grass (per fresh weight) for the given level of <sup>131</sup>I in air samples and given the assumed physico-chemical forms of <sup>131</sup>I present in the air. One possible explanation is that the fresh vegetation was actually very dry during September 1963. Another explanation is that the fraction of elemental iodine present in air could have been higher than specified in the scenario and higher than indicated by later experiments. To predict the concentrations in pasture grass the fraction of the elemental iodine in air given in the scenario was used without any modifications, and the dry-to-wet conversion factor was set to a value that is high (i.e., 33% kg<sub>dry</sub> kg<sub>fresh</sub><sup>-1</sup>; low content of water in the plants), but consistent with the local conditions.

The measured concentrations in milk at a given location were low, given the high concentrations in fresh pasture grass at the same location. This indicates that either an important fraction of their diet could have been uncontaminated stored feed (e.g., grains), or the cows in the region exhibit a low feed-to-milk transfer coefficient. The scenario however, states that the cows consumed mostly fresh pasture grass during September 1963. Thus, acceptable concentrations in milk are obtained by using a value for  $F_m$  closer to the lower bound of the  $F_m$  values reported in the literature, but consistent with experimental findings indicating lower transfer into milk during fall season (Lengemann et al. 1957).

The predicted time-dependent concentrations of <sup>131</sup>I in pasture grass and milk obtained using the adjusted parameter values are presented in Fig. 3 for Farm A—Benton City, Farm B—Twin Bridges, and Farm T—Pasco. For these locations the calculations

were started with the concentration of <sup>131</sup>I in air measured at nearby locations. The predictions reproduce well the measured concentrations in grass during the first half of the month but have a tendency to underestimate the observed concentrations in the second part of the month. The observed concentrations in grass in the second part of the month are also in discordance with the observed concentrations in milk during the same period of time (i.e., the concentration in grass is too high while the concentration in milk is too low, as compared to the first part of the month). This situation raises the issue of possible changes in the diet of the cows toward the end of the month (e.g., cows consumed more uncontaminated feed). The model used in this study was not designed to allow adjustments of the feed ingestion rates or the  $F_m$  values on a daily (or weekly) basis. Thus, the predictions presented here are obtained by setting the feed ingestion rate ( $Q_m$ ) and the  $F_m$  values and applying them for the entire month. Time-dependent  $Q_m$  and  $F_m$  values could be used, and the model predictions would change so that they would perfectly fit the observations at any location. However, such an exercise is pointless without information to indicate that such changes were appropriate; the usual practice is to use long-term averages for these (and other) parameter values.

The model has a tendency to underestimate the time-integrated concentrations in pasture grass (Fig. 4), so that the predicted concentrations for most sites are slightly lower than or equal to the observed values. On the other hand, the time-integrated concentrations in milk are equal to or slightly higher than the observed values. All observations, however, are contained within the predicted uncertainty ranges.

### Predicted <sup>131</sup>I thyroid burden activities in the thyroid glands and thyroid doses for two children on Farm B

Measurements of the activity content of the thyroid were taken on 19 October 1963, for a 4-y-old boy and an 8-y-old girl living on Farm B (Twin Bridges). The thyroid burden for the boy was 2.7 Bq, while the thyroid burden for the girl was below the limit of detection of 1 Bq (IAEA 2003; Soldat 1965). The children consumed milk from the cows raised on their farm. Reportedly, the average milk consumption rates are 1 gal per day (3.78 L d<sup>-1</sup>) for the boy and 1 quart per day (0.95 L d<sup>-1</sup>) for the girl. The rate for the boy (which was verified numerous times with the family of the children) is very high compared to the U.S. average consumption rates (Table 2). The rate for the girl is also high, being very close to the upper bound normally used in the *SENES* model (Table 2).

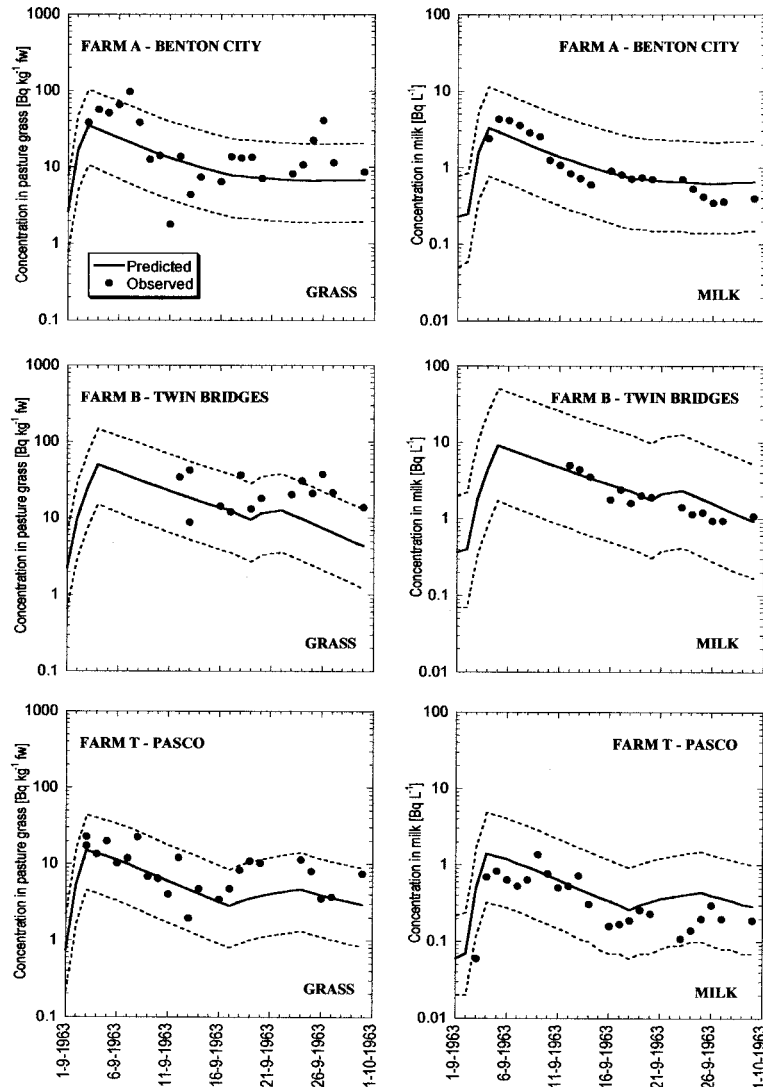
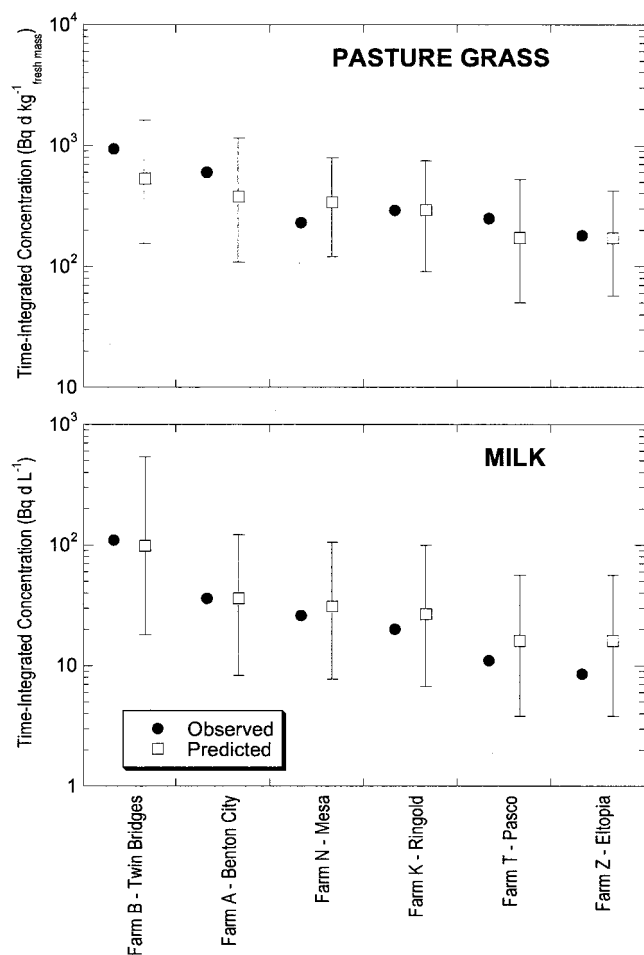


Fig. 3. Time-dependent concentrations of  $^{131}\text{I}$  in pasture grass and milk (at time of milking) for selected locations. The dotted lines represent the upper and lower bounds of the 95% confidence intervals of the predicted concentrations.

The *SENES* model predicted a thyroid burden for the 4-y-old boy of 5.1 Bq (95% CI = 2.3–11.3 Bq) for 19 October 1963. The observed activity in the thyroid of 2.7 Bq is contained in the 95% confidence interval, but the predicted central value is larger by about a factor of 2. These predictions were obtained assuming no releases of  $^{131}\text{I}$  occurred after 1 October 1963 (which might not be correct since the PUREX plant was still functioning). Assuming that the reported ingestion rate is correct, the overestimation could be due to the application of a thyroid model designed for the average member of the population. The model used here has an assumed fractional uptake of iodine from blood into the thyroid gland of 36% (Apostoaiei and Miller 2004), which is comparable to the fractional uptake of 30% proposed by the ICRP (Publication 67; ICRP 1993). Given that milk is also one

of the sources of stable iodine (ICRP 1975), a child consuming large amounts of milk on a regular basis will have the thyroid gland almost saturated with iodine, thus presenting a low transfer of iodine from blood into the thyroid gland. If a fractional uptake of 20% were used for the 4-y-old boy, the predicted thyroid burden would be 2.65 Bq (95% CI 1.2–5.9 Bq), which would match the observed value.

For the 8-y-old girl, the model predicted an activity in the thyroid of 1.4 Bq (95% CI = 0.3–6.6 Bq), on 19 October 1963. The observed thyroid burden of 1 Bq or less is probably contained in the 95% confidence interval. The amount of overestimation in the central value is not known. Applying the same logic as for the 4-y-old boy, a fractional uptake of 20% would predict a thyroid burden below 1 Bq (i.e., 0.9 Bq; 95% CI = 0.19–4.2 Bq).



**Fig. 4.** Predicted time-integrated concentrations in pasture grass and milk (at time of milking). The vertical lines represent the 95% confidence intervals of the predicted concentrations.

The predicted thyroid doses for the boy and the girl are 0.94 mSv (95% CI = 0.13–7.1 mSv) and 0.13 mSv (95% CI = 0.017–1.1 mSv), respectively. If the blood-to-thyroid fractional transfer is lowered as described above, the doses for the boy and the girl become 0.49 mSv (95% CI = 0.0062–3.6 mSv) and 0.087 mSv (95% CI = 0.012–0.66 mSv).

**Predicted thyroid doses for representative individuals**

Thyroid doses were predicted for representative individuals of various ages at exposure and both sexes. Fig. 5 shows doses estimated for representative individuals at Farm A—Benton City. The largest doses from ingestion of milk occur for 1-y-old children. Even though infants have the largest dose coefficient (Table 4), they drink less cow’s milk than 1-y-old children, and thus they have slightly lower thyroid doses from ingestion of cow’s milk. Sex differences are observed starting with exposure at age 15 y, because teenage and adult females consume less milk than males of similar ages. The

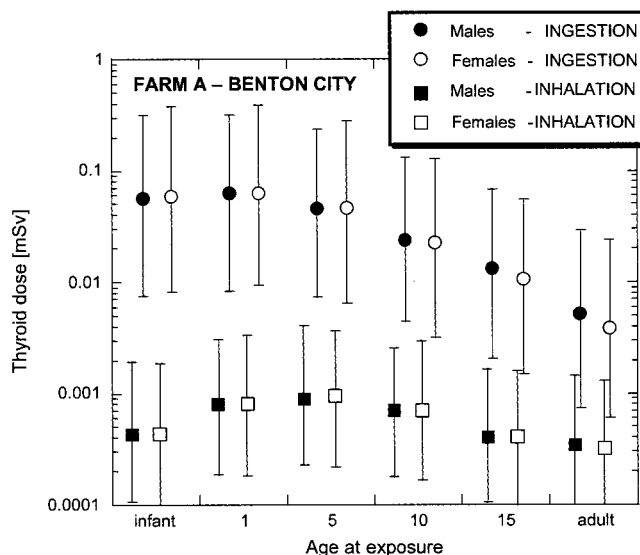


**Fig. 5.** Thyroid doses from ingestion of cow’s milk and from inhalation for representative individuals living on Farm A—Benton City. The vertical lines represent the 95% confidence intervals of the predicted doses.

breathing rates increase with age, while the dose coefficients decrease with age, so that the maximum inhalation doses are obtained for children exposed around 5 y of age (Fig. 5).

**Predicted excess lifetime risk of thyroid cancer**

The excess lifetime risk of thyroid cancer varies by a factor of 6.5 between the location of the highest predicted exposure (Farm B—Twin Bridges) and the location with the lowest predicted exposure (Farm T—Pasco). The risk for females is more than two times larger than the risk for males (Fig. 6) because females exhibit a higher sensitivity to radiation and a higher incidence of thyroid cancer due to natural causes (Apostoaei et al. 2003b). The highest risk is estimated for newborns and 1-y-old children; the risk decreases with age due to the decrease with age of the dose and risk factors. The risk for adults is about two orders of magnitude lower than the risk for young children.

The excess lifetime risk for the 4-y-old boy at Farm B was estimated as  $1.1 \times 10^{-5}$  (95% C.I.  $9.8 \times 10^{-7}$ – $1.3 \times 10^{-4}$ ). For the 8-y-old girl the predicted risk at Farm B is  $3.0 \times 10^{-6}$  (95% C.I.  $2.4 \times 10^{-7}$ – $3.2 \times 10^{-5}$ ). If the blood-to-thyroid fractional transfer is lowered as described above, the predicted risk for the 4-y-old boy is  $6.2 \times 10^{-6}$  (95% C.I.  $5.0 \times 10^{-7}$ – $6.2 \times 10^{-5}$ ), while the predicted risk for the 8-y-old girl is  $2.0 \times 10^{-6}$  (95% C.I.  $1.9 \times 10^{-7}$ – $2.1 \times 10^{-5}$ ).

**Sensitivity analysis**

A sensitivity analysis was conducted to determine the most important contributors to the uncertainty in the

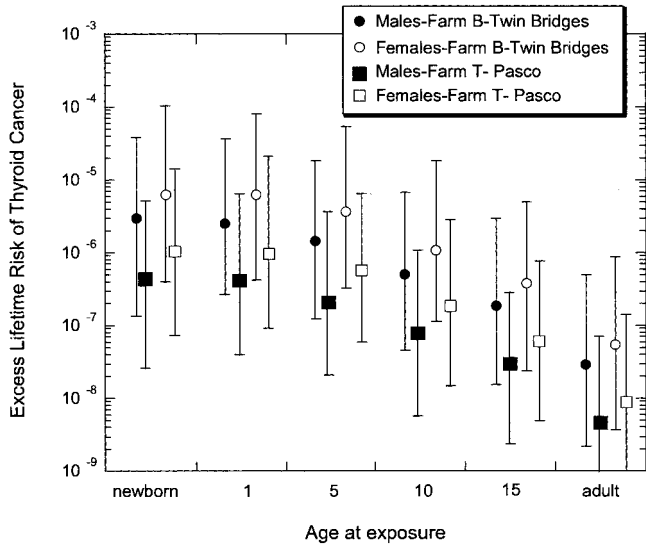


**Fig. 6.** Excess Lifetime Risk (ELR) of thyroid cancer for representative individuals living on Farm B—Twin Bridges (largest predicted exposures) and on Farm T—Pasco (lowest predicted exposures). The vertical lines represent the 95% confidence intervals of the predicted risks.

estimated excess lifetime risk of thyroid cancer. Fig. 7 shows the results of the sensitivity analysis for a 1-y-old female. The risk factor (ELR Sv<sup>-1</sup>) has the largest contribution to the uncertainty, followed by the dose coefficient, the feed-to-milk transfer coefficient, the concentration <sup>131</sup>I in air, and parameters describing the deposition of elemental iodine onto the ground. These results apply to other ages at exposure and to both sexes, because the magnitude of the uncertainty in the most important parameters does not depend significantly on age or sex.

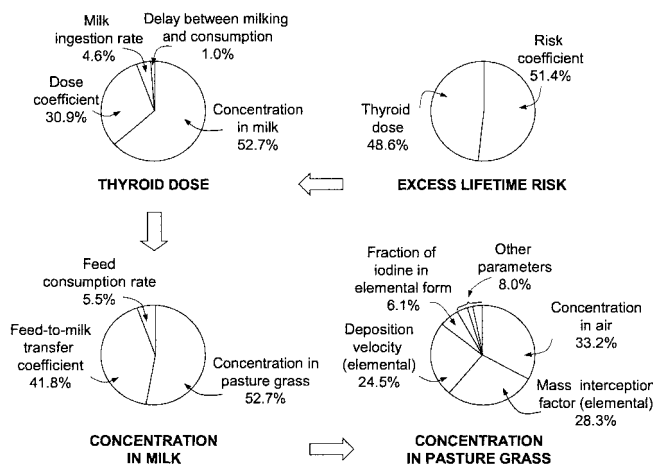


**Fig. 7.** Results of a sensitivity analysis showing the main contributors to the uncertainty in quantities estimated in each step of the calculation. Results are for a 1-y-old female at Farm A—Benton City.

**A comparison with predictions made by other modelers**

Results produced for Farm B (Twin Bridges) are used to compare the *SENES* model with models used in the IAEA BIOMASS program (IAEA 2003). This location was selected for inter-model comparison because it received the highest deposition of <sup>131</sup>I and because it is the location for which measurements of <sup>131</sup>I activity in thyroid glands of real individuals are available.

For all modelers other than Napier and Homma (2), the best estimates of <sup>131</sup>I time-integrated concentration in pasture grass at Farm B are within a factor of two of the measured concentration, and within a factor of 3 among themselves (Fig. 8). The concentration produced by the *SENES* model is lower by a factor of 1.8 than the observed concentration. Most modelers estimated uncertainty ranges on the predicted concentration in pasture grass that contain the measured concentration.

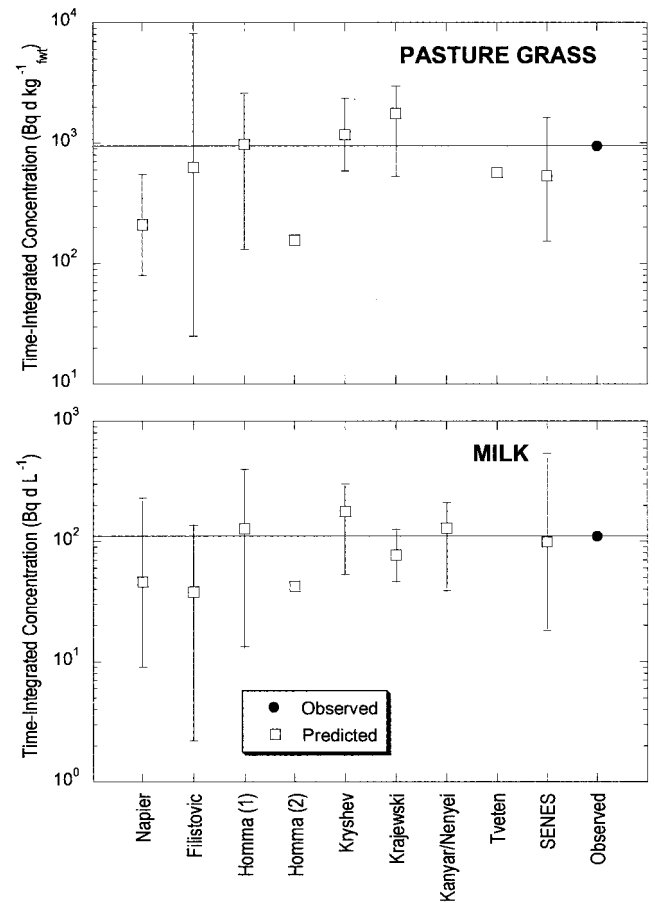


**Fig. 8.** Comparison of time-integrated concentrations in pasture grass and milk at Farm B (Twin Bridges) predicted by various modelers (IAEA 2003) and in this study. The vertical lines represent the uncertainty range provided by each modeler. For predictions using the *SENES* model, the vertical lines represent the 95% confidence intervals of the predicted concentrations. Homma (1) and (2) represent two sets of results reported by Homma as described in Table 1.

The predicted time-integrated concentrations in milk at Farm B are within a factor of 3 of the measured concentration and within a factor of 5 among themselves (Fig. 8). The *SENES* model produced a concentration in milk only 10% different from the observed concentration.

All ingestion doses predicted for people exposed as adults are within a factor of 2 of each other, with the exception of doses predicted by Homma (2) and Kanyar/Nenyai (Fig. 9). The low doses predicted by Homma (2) are due to the overall low predictions for all endpoints produced by this modeling approach (Fig. 8). Given that the concentration in milk estimated by Kanyar/Nenyai was very close to the measured concentration (Fig. 8), their high dose estimate (Fig. 9) is probably due to a high dose coefficient and to ignoring the delay between milking and consumption.<sup>§</sup>

Ingestion doses for individuals exposed as infants estimated using the *SENES* model are similar to those estimated by Krajewski, and a factor of 4 larger than doses estimated by Filistovic and Kryshev. The later two participants estimated lower doses to infants because they used a dose coefficient designed for adult exposures. Moreover, Filistovic's low dose estimate is also due to an underestimation of the concentration in milk (Fig. 8).

Two sets of ingestion doses were produced using the *SENES* model for the two children who lived on Farm B—Twin Bridges (Fig. 10). The first set assumes default ingestion dose coefficients, while the second set uses lower dose coefficients determined assuming partial saturation of the thyroid gland due to consistently high milk consumption rates by the two children. Doses estimated by *SENES* for the two children are similar to those estimated by Krajewski, Napier, and Kryshev. Filistovic produced lower dose estimates due to the same reasons explained above. The doses estimated by Napier and Kryshev show the effect of compensatory biases. That is, Napier underestimated the concentration in milk (Fig. 8), but he probably used a relatively high dose coefficient. Conversely, Kryshev's model has a tendency to overestimate the concentration in milk (Fig. 8), but he used a dose coefficient designed for adults that is low when applied for 4-y-old and 8-y-old children.

Doses estimated using the *SENES* model have wider confidence ranges than doses predicted by other models (Fig. 9 and 10) because the *SENES* model quantifies the uncertainty in all parameters including ingestion and breathing rates and dose coefficients. As shown by the sensitivity analysis performed in this study, more than 30% of the uncertainty in the estimated doses is due to the uncertainty in the dose coefficients (Fig. 7). None of

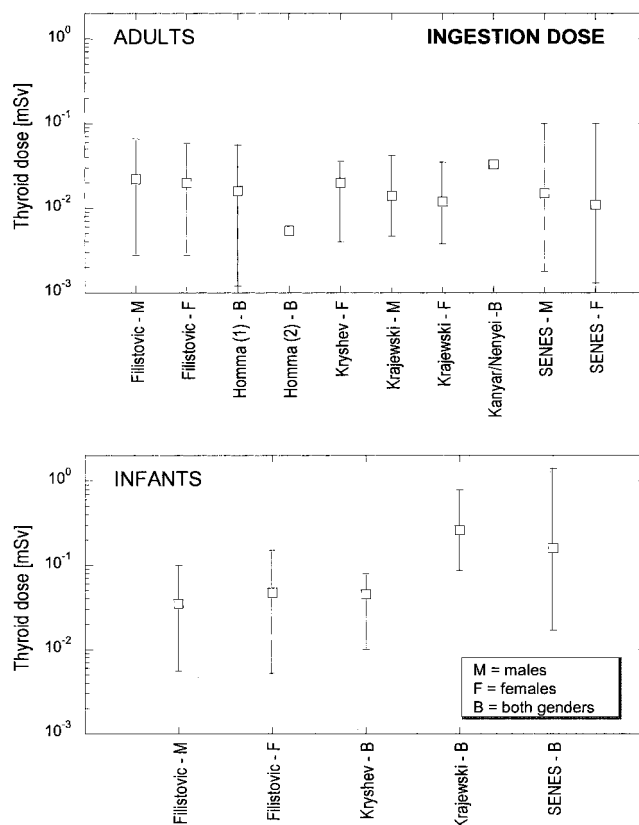


**Fig. 9.** Comparison of thyroid doses from ingestion of  $^{131}\text{I}$  by representative individuals at Farm B (Twin Bridges) as estimated by various modelers (IAEA 2003) and in this study. The vertical lines represent the uncertainty range provided by each modeler. For predictions using the *SENES* model, the vertical lines represent the 95% confidence intervals of the predicted doses.

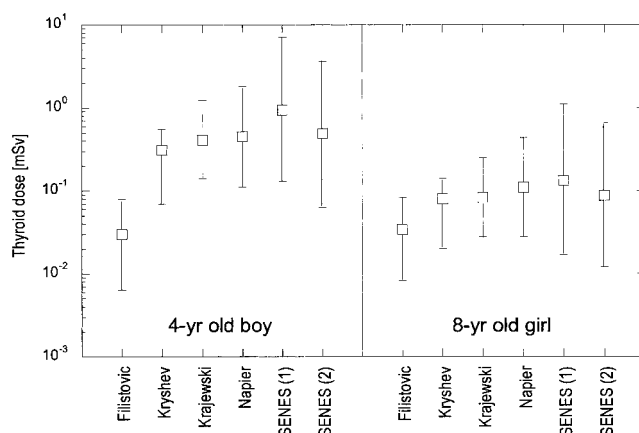


**Fig. 10.** Comparison of thyroid doses from ingestion of  $^{131}\text{I}$  for two children who lived on Farm B (Twin Bridges) estimated by various modelers (IAEA 2003) and in this study. Predictions labeled *SENES* (1) were obtained using default ingestion dose coefficients. Predictions labeled *SENES* (2) were obtained using lower dose coefficients determined assuming partial saturation of the thyroid gland due to consistently high milk consumption rates by the two children. The vertical lines represent the uncertainty range provided by each modeler. For predictions using the *SENES* model, the vertical lines represent the 95% confidence intervals of the predicted doses.

<sup>§</sup> No details are provided by Kanyar/Nenyai for these parameters (IAEA 2003).

the other modelers included uncertainties in the dose coefficients, and many of them quantified the uncertainties on only a limited number of parameters of their models (IAEA 2003). One participant (Kryshev) estimated uncertainty ranges in doses by using professional judgment, and some participants did not report uncertainties for some of the dose endpoints.

### A discussion of the transfer of $^{131}\text{I}$ from feed to milk of dairy cows around Hanford

As mentioned before, the measured concentrations in milk at a given location are strangely low, relative to concentrations in fresh pasture grass observed at the same location. To further investigate this issue, site-specific  $F_m$  values were derived after the model testing was completed (and they were not used in the modeling described in this paper). The  $F_m$  values were obtained using the measured time-integrated concentrations of  $^{131}\text{I}$  in milk and in pasture grass measured around Hanford. In derivation of the  $F_m$  values, it was assumed that cows consumed fresh pasture grass at the rates reported in the scenario (around  $9 \text{ kg}_{\text{dry mass}} \text{ d}^{-1}$  for backyard cows, and around  $8.5 \text{ kg}_{\text{dry mass}} \text{ d}^{-1}$  for commercial cattle; see Methods section for probability distributions), that the measured concentrations in pasture grass are indeed reported per fresh mass, and that the content of water in grass plants can be described by a dry-mass to fresh-mass conversion factor uniformly distributed from 0.2 to 0.45  $\text{kg}_{\text{dry mass}} \text{ kg}^{-1}_{\text{fresh mass}}$ . For Farm B, where most likely the cows were managed as “backyard” cows, the  $F_m$  was  $0.0039 \text{ d L}^{-1}$  (95% C.I.  $0.0021\text{--}0.0060 \text{ d L}^{-1}$ ). For the rest of the farms, where most likely the cows were managed as “commercial” cows, the average  $F_m$  was  $0.0022 \text{ d L}^{-1}$  (95% C.I.  $0.0013\text{--}0.0034 \text{ d L}^{-1}$ ). These values are low compared to the  $F_m$  values observed elsewhere and normally used in dose reconstruction studies (Apostoaie et al. 1999a, 2003a; NCI 1997), including in the Hanford Environmental Dose Reconstruction (HEDR; Snyder et al. 1994). This issue is especially important because the HEDR study used much larger  $F_m$  values to predict doses from 1944–1957 releases of  $^{131}\text{I}$  from the Hanford chemical processing plant (backyard cow  $F_m = 0.0092 \text{ d L}^{-1}$  with a 95% CI  $0.0016\text{--}0.052 \text{ d L}^{-1}$  and commercial cow  $F_m = 0.012 \text{ d L}^{-1}$  with a 95% C.I. of  $0.0073\text{--}0.016 \text{ d L}^{-1}$ ; Snyder et al. 1994).

However, this finding does not automatically lead to the conclusion that doses estimated in the HEDR study are overestimated due to a high  $F_m$ . For instance, HEDR model was used in the BIOMASS Hanford exercise by B. Napier (one of its developers; IAEA 2003). HEDR predictions in the Hanford exercise indicate an underestimation of the concentration of  $^{131}\text{I}$  in both vegetation and

milk, even though HEDR was apparently run using default (i.e., high-sided)  $F_m$  values of  $0.092 \text{ d L}^{-1}$  for backyard cows and  $0.012 \text{ d L}^{-1}$  for commercial cows (IAEA 2003; Snyder et al. 1994).

## SUMMARY AND CONCLUSION

A model describing transport of  $^{131}\text{I}$  in the environment that was developed by *SENES* Oak Ridge, Inc., for assessment of radiation doses and excess lifetime risk from releases of radioactivity from Oak Ridge Reservation in Oak Ridge, TN, and from Idaho National Engineering Environmental Laboratory (INEEL) in southeast Idaho, was tested using environmental data collected in September 1963 after an accidental release into the atmosphere of 2.33 TBq (63 Ci) of  $^{131}\text{I}$  from the Hanford PUREX Chemical Separations Plant, in Hanford, WA. An additional 0.33 TBq (9 Ci) were released until the end of September 1963 for a total of 2.66 TBq (72 Ci). Data assembled by IAEA’s BIOMASS program (IAEA 2003) allowed testing of the *SENES* model for various endpoints (i.e., accumulation in vegetation, milk, and human thyroid glands). The *SENES* model was first calibrated and then applied to all locations without fitting the model parameters for a given location.

The predicted concentrations in vegetation and milk showed that the *SENES* model reproduces satisfactorily both the time-dependent and time-integrated measured concentrations in pasture grass and milk. The time-integrated concentrations in grass and milk are within a factor of 2 of the observed values, and the time-dependent concentrations reproduce the temporal pattern and magnitude of the daily measured concentrations in grass and milk.

This model was also able to predict the activity of  $^{131}\text{I}$  in the thyroid glands of two children. Initial predictions were within a factor of two of the measured activities, when the model was used without adjustments for any parameter of the internal dosimetry model. When the transfer of  $^{131}\text{I}$  from blood to thyroid was adjusted downwards based on the allegedly high stable iodine consumption of the children, the thyroid burdens were predicted within a few percent. These results are encouraging given that the observed activity in the thyroid glands of the two children was quite low, because measurements were performed at a late date (47 d after the accident), by which time most of the  $^{131}\text{I}$  had decayed.

A model intercomparison showed that the *SENES* model produces results consistent with predictions generated by various models used in the BIOMASS Hanford modeling exercise (IAEA 2003). However, as opposed to other models employed with this data set, the *SENES*

model quantifies uncertainties in the estimated doses and risks in a rigorous manner, by accounting for uncertainties in each model parameter and by using Monte Carlo methods for propagation of uncertainties.

A sensitivity analysis showed that the uncertainty in the thyroid dose coefficients contributes more than 30% of the uncertainty in estimated <sup>131</sup>I doses. Since no previous modelers quantified the uncertainties in the dose coefficients, the confidence intervals of doses estimated by their models are too narrow and do not reflect the full state of knowledge about estimated doses. Other major sources of uncertainty in estimated doses include the predicted or measured concentrations of <sup>131</sup>I in air from which the model starts, the values of the mass interception factor and deposition velocity for elemental iodine (which affect the predicted <sup>131</sup>I concentration in grass), and the feed-to-milk transfer coefficient (which affects the predicted <sup>131</sup>I concentration in milk). The uncertainty in the estimated thyroid doses and the uncertainty in the risk factors contribute almost equally to the uncertainty in the final estimate of risk.

The exposure to the 1963 PUREX/Hanford accident produced low doses and risks to the people living at the studied locations. The upper 97.5th percentile of the excess lifetime risk of thyroid cancer for the most extreme situation is about 10<sup>-4</sup>.

*Acknowledgments*—This work was funded, in part, by the Centers for Disease Control and Prevention under Grant R32/CCR416742-02. The author is grateful to Kathleen M. Thiessen of SENES Oak Ridge, Inc., for providing access to IAEA published materials, as well as for the technical review and editing of this paper.

## REFERENCES

- Aoyama M, Hirose K, Suzuki Y, Inoue H, Sugimura Y. High level radioactive nuclides in Japan in May. *Nature* 321:819–820; 1986.
- Apostoaie AI, Miller LF. Uncertainties in the dose coefficients from ingestion of I-131, Cs-137, and Sr-90. *Health Phys* 86:460–482; 2004.
- Apostoaie AI, Burns RE, Hoffman FO, Ijaz T, Lewis CJ, Nair SK, Widner TE. Iodine-131 releases from Radioactive Lanthanum processing at the X-10 site in Oak Ridge, Tennessee (1944–1956)—An assessment of quantities released, off-site radiation doses, and potential excess risks of thyroid cancer. The report of Project Task 1. Oak Ridge, TN: Tennessee Department of Health Oak Ridge Health Studies, Oak Ridge Dose Reconstruction; Vols. 1 and 1A; 1999a.
- Apostoaie AI, Blaylock BG, Caldwell B, Flack S, Gouge JH, Hoffman FO, Lewis CJ, Nair SK, Reed EW, Thiessen KM, Thomas BA, Widner TE. Radionuclides released to the Clinch River from White Oak Creek on the Oak Ridge Reservation—An assessment of historical quantities released, off-site radiation doses, and health risks. A report of the Oak Ridge Dose Reconstruction, Vols. 4 and 4A. The report of Project Task 4. Oak Ridge, TN: Tennessee Department of Health, Oak Ridge Health Studies, Oak Ridge Dose Reconstruction; 1999b.
- Apostoaie AI, Thomas BA, Kocher DC, Hoffman FO. Doses to the public from atmospheric releases of radionuclides from the Idaho Chemical Processing Plant at Idaho National Engineering Laboratory (1957–1959). A report to the Centers for Disease Control and Prevention. Oak Ridge, TN: SENES Oak Ridge, Inc.; McLean, VA: S. Cohen and Associates; 2003a.
- Apostoaie AI, Thomas BT, Hoffman FO, Nieman T. Technical documentation of the iodine-131 thyroid dose and risk calculator for Nevada Test Site fallout. A SENES Oak Ridge, Inc., report for the National Cancer Institute, Division of Epidemiology and Genetics, Radiation Epidemiology Branch. Oak Ridge, TN: SENES Oak Ridge, Inc; 2003b.
- Bondiotti EA, Brantley JN. Characteristics of Chernobyl radioactivity in Tennessee. *Nature* 322:313–314; 1986.
- Brown J, Goossens LHM, Kraan BCP, Cooke RM, Harper FT, Haskin FE, Abbott ML, Young ML, Hora SC, Rood A. Probabilistic accident consequence uncertainty analysis. Food chain uncertainty analysis. Luxembourg: Office of Publications of the European Communities; NUREG/CR-6523; EUR 16771; SAND97-0335; 1997.
- Bunch DF. Controlled environmental radioiodine tests. Progress report number two. Idaho Falls, ID: U.S. Atomic Energy Commission, Idaho Operations Office; AEC Research and Development Report IDO-12053; 1966.
- Bunch DF. Controlled environmental radioiodine tests. Idaho Falls, ID: U.S. Atomic Energy Commission, Idaho Operations Office; Progress Report Number Three. AEC Research and Development Report IDO-12063; 1968.
- Cambray RS, Cawse PA, Garland JA, Gibson AB, Johnson P, Lewis GN, Newton D, Salmon L, Wade BO. Observations on radioactivity from the Chernobyl accident. *Nuclear Energy* 26:77–101; 1987.
- Chamberlain AC. Aspects of the deposition of radioactive and other gases and particles. *Int J Air Pollut* 3:63–68; 1960.
- Chamberlain AC, Chadwick RC. Deposition of airborne radioiodine vapour. *Nucleonics* 11:22–25; 1953.
- Chamberlain AC, Chadwick RC. Transport of iodine from the atmosphere to ground. *Tellus* 18:226–237; 1966.
- Decisioneering. Crystal Ball risk analysis software. Professional edition. Version 5.2. Denver, CO: Decisioneering, Inc; 2000. Available at [www.crystalball.com](http://www.crystalball.com). Accessed 26 January 2005.
- Hawley CA Jr, Sill CW, Voelz GL, Isplitzer NF. Controlled environmental radioiodine tests at the National Reactor Testing Station. Idaho Falls, ID: U.S. Atomic Energy Commission, Idaho Operations Office; US AEC report IDO-12035; 1964.
- Heinemann K, Vogt KJ. Measurements of the deposition of iodine onto vegetation and of the biological half-life of iodine on vegetation. *Health Phys* 39:463–474; 1980.
- Hoffman FO. A review of measured values of the milk transfer coefficient (Fm) for iodine. *Health Phys* 35:413–416; 1978.
- Hoffman FO, Baes CF III. A statistical analysis of selected parameters for predicting food chain transport and internal dose of radionuclides. Oak Ridge, TN: Oak Ridge National Laboratory; NUREG/CR-1004, ORNL/NUREG/TM-282; 1979.
- Iman R, Shortencarier MJ. A FORTRAN-77 program and user's guide for generation of Latin Hypercube Sampling and random sampling for use with computer models. Albuquerque, NM: Sandia National Laboratory; U.S. Nuclear Regulatory Commission; NUREG/CR-3624; 1984.

- International Atomic Energy Agency. Testing of environmental transfer models using data from the atmospheric release of iodine-131 from the Hanford site, USA, in 1963. Report of Dose Reconstruction Working Group of the Biosphere Modelling and Assessment (BIOMASS) Programme, Theme 2. Biosphere Modelling and Assessment Methods (BIOMASS) programme. Vienna: IAEA; IAEA-BIOMASS-2; 2003. Available at [www-pub.iaea.org/MTCD/publications/publications.asp](http://www-pub.iaea.org/MTCD/publications/publications.asp). Accessed October 2004.
- International Commission on Radiological Protection. Report of the Task Group on Reference Man. Oxford: Pergamon Press; ICRP Publication 23; 1975.
- International Commission on Radiological Protection. Age-dependent doses to members of the public from intake of radionuclides: Part 2, Ingestion dose coefficients. Oxford: Pergamon Press; ICRP Publication 67, Ann ICRP 23(3/4); 1993.
- International Commission on Radiological Protection. Age-dependent doses to members of the public from intake of radionuclides: Part 5, Compilation of ingestion and inhalation coefficients. Oxford: Pergamon Press; ICRP Publication 72, Annals of the ICRP Vol 26; 1996.
- International Commission on Radiological Protection. Database of dose coefficients: Workers and members of the public. Version 2.0.1. Oxford: Pergamon Press; 2000.
- Kohler H, Peterson SR, Hoffman FO. Multiple model testing using Chernobyl fallout data of I-131 in forage and milk and <sup>137</sup>Cs in forage, milk, beef and grain. Stockholm: National Institute of Radiation Protection; Biospheric Model Validation Study (BIOMOVS) Technical Report 13; 1991.
- Koranda JJ. Agricultural factors affecting the daily intake of fresh fallout by dairy cows. Biology and medicine, UC-48. TID-4500. Livermore, CA: University of California; Lawrence Radiation Laboratory; UCRL-12470; 1965.
- Krasner-Khait B. The impact of refrigeration. History Magazine (February-March) 2000. Available at <http://www.history-magazine.com/refrig.html>. Accessed 24 January 2005.
- Land C, Gilbert E, Smith J, Hoffman FO, Apostoaei IA, Thomas BA, Kocher DC. Report of the NCI-CDC Working Group to revise the 1985 NIH Radioepidemiological Tables. Bethesda, MD: U.S. Department of Health and Human Services, National Institutes of Health, National Cancer Institute; 2003.
- Lengemann FW, Swanson EW, Monroe RA. Effect of season on secretion of iodine in milk. *J Dairy Sci* 40:387-393; 1957.
- Ludwick JD. Investigation of the nature of I-131 in the atmosphere. In: Gamertsfelder CC, Green JK, eds. Hanford Radiological Sciences Research and Development Annual Report for 1963. Richland, WA: General Electric Co., Hanford Atomic Products Operation; HW-81746; 1964.
- Ludwick JD. A portable boom-type air sampler. In: Pearce DW, Compton MR, eds. Pacific Northwest Laboratory Annual Report for 1966 to the USAEC Division of Biology and Medicine. Vol. II: Physical Sciences, Part 1, Atmospheric sciences. Richland, WA: Pacific Northwest Laboratory; BNWL-481 1; 1967: 87-92.
- Morgan MG, Henrion M. A guide to dealing with uncertainty in quantitative risk and policy analysis. New York: Cambridge University Press; 1990.
- Mueck K. Variations in activity concentration and radionuclide ratio in air after the Chernobyl accident and its relevance to inhalation dose estimates. *Radiat Protect Dosim* 22:219-229; 1988.
- National Cancer Institute. Estimated exposure and thyroid doses received by the American people from iodine-131 fallout following Nevada atmospheric nuclear bomb tests. Bethesda, MD: U.S. Department of Health and Human Services; National Institutes of Health, National Cancer Institute; 1997.
- Perkins RW. Studies of radioiodine and other fallout radionuclides in air. In: Gamertsfelder C, Green JK, eds. Hanford Radiological Sciences Research and Development Annual Report for 1962. Richland, WA: General Electric Co., Hanford Atomic Products Operation; HW-77609; 1963: 3.36-3.48.
- Perkins RW. Physical and chemical forms of I-131 from fallout and chemical processing plants. In: Gamertsfelder CC, Green JK, eds. Hanford Radiological Sciences Research and Development Annual Report for 1963. Richland, WA: General Electric Co., Hanford Atomic Products Operation; HW-81746; 1964: 3.55-3.58.
- Ramsdell JV Jr, Simonen CA, Burk KW. Regional atmospheric transport code for Hanford emission tracking (RATCHET). Hanford Environmental Dose Reconstruction Project. Richland, WA: Battelle Pacific Northwest Laboratories; PNWD-2224 HEDR, UC-000; 1994.
- Schwartz G, Hoffman FO. Imprecision of dose predictions for radionuclides released to the environment: An application of a Monte Carlo simulation technique. *Environment Internat* 4:289-297; 1980.
- Simon SL, Lloyd RD, Till JE. Development of a method to estimate thyroid dose from fallout radioiodine in cohort study analyses and modeling internal dose estimates. *Health Phys* 59:669-691; 1990.
- Snyder SF, Farris WT, Napier BA, Ikenberry TA, Gilbert RO. Parameters used in the environmental pathways and radiological dose modules (DESCARTES, CIDER, and CRD Codes) of the Hanford Environmental Dose Reconstruction Integrated Codes (HEDRIC). Richland, WA: Battelle Pacific Northwest Laboratories; PNWD-2033 HEDR Rev. 1; 1994.
- Soldat JK. Environmental evaluation of an acute release of <sup>131</sup>I to the atmosphere. *Health Phys* 11:1009-1015; 1965.
- Thiessen KM, Napier BA, Filistovic V, Homma T, Kanyar B, Krajewski P, Kryshev AI, Nedveckaite T, Nenyeyi A, Sazykina TG, Tveten U, Sjoblom K-L, Robinson C. Model testing using data from accidental releases of I-131 and Cs-131. 1: Model testing using data on I-131 released from Hanford. In: Proceedings from the International Conference on Radioactivity in the Environment. 2002: 313-316.
- Thiessen KM, Napier BA, Filistovic V, Homma T, Kanyar B, Krajewski P, Kryshev AI, Nedveckaite T, Nenyeyi A, Sazykina TG, Tveten U, Sjoblom K-L, Robinson C. Model testing using data on I-131 released from Hanford. *J Environmental Radioact* (in press).
- Till JE, Meyer RH, eds. Radiological assessment: A textbook on environmental dose analysis. Oak Ridge, TN: Oak Ridge National Laboratory; ORNL-5968; 1983.
- Voilleque PG. Iodine species in reactor effluents and in the environment. Palo Alto, CA: Electric Power Research Institute; EPRI-NP-1269; 1979.